Article:

Bijkerk, JF, Eggenhuisen, JT, Kane, IA et al. (4 more authors) (2016) Fluvio-Marine Sediment Partitioning as a Function of Basin Water Depth. Journal of Sedimentary Research, 86 (3). pp. 217-235. ISSN 1527-1404

https://doi.org/10.2110/jsr.2016.9

RUNNING HEAD:

WATER-DEPTH CONTROL ON FLUVIO-MARINE SEDIMENT PARTITIONING

TITLE:

FLUVIO-MARINE SEDIMENT PARTITIONING AS A FUNCTION OF BASIN WATER DEPTH

JOCHEM. F. BIJKERK[1,3], JORIS T. EGGENHUISEN[2], IAN A. KANE[4], NIELS MEIJER[2], COLIN N. WATERS[3], PAUL B. WIGNALL[1], WILLIAM D. MCCAFFREY[1]

1) School of Earth and Environment, University of Leeds, Leeds LS2 9JT, UK

2) Department of Earth Sciences, Utrecht University, PO Box 80021, 3508 TA Utrecht, The Netherlands

3) British Geological Survey, Environmental Science Centre, Keyworth, Nottingham NG12 5GG, UK

4) School of Earth, Atmospheric and Environmental Sciences, University of Manchester, Manchester M13 9PL, UK

Email: jochem.j.bijkerk@shell.com

KEYWORDS (5x):

Analogue modeling, sequence stratigraphy, longitudinal profiles, downstream fining, water depth

1. ABSTRACT

Progradational fluvio-deltaic systems tend towards but cannot reach equilibrium, a state in which the longitudinal profile does not change shape and all sediment is bypassed beyond the shoreline. They cannot reach equilibrium because progradation of the shoreline requires aggradation along the longitudinal profile. Therefore progradation provides a negative feedback, unless relative sea level falls at a sufficient rate to cause non-aggradational extension of the longitudinal profile. How closely fluvio-deltaic systems approach equilibrium is dependent on their progradation rate, which is controlled by water depth and downstream allogenic controls, and governs sediment partitioning between the fluvial, deltaic, and marine domains. Here, six analogue models of coastal fluvio-deltaic systems and small prograding shelf margins are examined to better understand the effect of water depth, subsidence, and relative sea-level variations upon longitudinal patterns of sediment partitioning and grain-size distribution that eventually determine large-scale stratigraphic architecture. Fluvio-deltaic systems prograding in relatively deep-water environments are characterized by relatively low progradation rates compared to shallow-water systems. This allows these deeper water systems to approach equilibrium more closely, enabling them to construct less concave and steeper longitudinal profiles that provide low accommodation to fluvial systems. Glacio-eustatic sea-level variations and subsidence modulate the effects of water depth on the longitudinal profile. Systems are closest to equilibrium during falling relative sea level and early lowstand, resulting in efficient sediment transport towards the shoreline at those times. Additionally, the strength of the response to relative sea-level fall differs dependent on water depth. In systems prograding into deep water, relative sea-level fall causes higher sediment bypass rates and generates significantly stronger erosion than in shallow-water systems, which increases the probability of incised-valley formation. Water depth in the receiving basin thus forms a first-order control on the sediment partitioning along the longitudinal profile of fluvio-deltaic systems and the shelf clinoform style. It also forms a control on the availability of sand-grade sediment at the

shoreline that can potentially be remobilized and redistributed into deeper marine environments. Key findings are subsequently applied to literature of selected shelf clinoform successions.

2. INTRODUCTION

Understanding sediment partitioning between the fluvial, deltaic, and marine environments on geological time scales presents a major challenge in sedimentology and sequence stratigraphy (e.g., Bourget et al. 2013; Covault et al. 2011; Martinsen et al. 2010; Sømme et al. 2009). Sediment transport and its consequent depositional distribution along the longitudinal profile of alluvial rivers and delta systems can be understood through the concept of “equilibrium” or “grade” (Muto and Swenson 2005). Longitudinal profiles are generally concave up, their shape describing the decreasing gradient of alluvial river systems dependent on, e.g., geological structure, geomorphology, and water-discharge and sediment-discharge parameters (e.g., Sinha and Parker 1996; Rice and Church 2001). When longitudinal profiles are in equilibrium, all sediment is conveyed through the system without net erosion or deposition, implying that net sediment output is equal to sediment input, and thus that the shape of the longitudinal profile does not change (Fig. 1A).

Early morphological definitions of equilibrium and graded longitudinal profiles typically focus on small river segments over short time scales, and suggest that many rivers are in equilibrium (e.g., Mackin 1948; Schumm and Lichty 1965). Contrarily, Muto and Swenson (2005) suggest most fluvio-deltaic systems are in non-equilibrium because downstream deltaic deposition on geological time scales implies a lengthening of the longitudinal profile, which typically requires aggradation along this profile. Only during relative sea-level fall, non-aggradational extension of the fluvio-deltaic longitudinal profile is possible, which implies that equilibrium can be achieved (Muto and Swenson 2005). We refer to this concept of equilibrium as system-scale equilibrium to distinguish it from older definitions.

System-scale equilibrium of fluvio-deltaic systems in sedimentary basins is typically in the order of 10^5 to 10^6 y (Paola et al. 1992a), and is approached asymptotically (Postma et al. 2008). Analogue and numerical modeling shows that fluvio-deltaic systems that are far removed from equilibrium approach this state rapidly by using a large percentage of the sediment load for aggradation of the fluvial system (Postma et al. 2008). Conversely, systems that are close to equilibrium conditions develop towards this state more slowly using a small percentage of the available sediment load while most sediment is bypassed beyond the shoreline. How closely systems approaches system-scale equilibrium thus controls the sediment volume used for aggradation along the longitudinal profile and the sediment volume available for progradation of the shoreline. This represents a negative feedback mechanism in which the magnitude of the departure from system-scale equilibrium (Voller and Paola 2010) determines fluvio-marine sediment partitioning, thereby setting the progradation rate, which determines the departure from system-scale equilibrium (Fig. 1B).

Water depth forms a primary control on progradation rate and might thus influence aggradation rates along the longitudinal profile via the above-described feedback mechanism. Additionally, relative sea-level variations can significantly affect shoreline migration rates as well as the position of the equilibrium profile relative to the actual longitudinal profile of coastal fluvio-deltaic systems (Wheeler 1964). This is used in sequence-stratigraphic models to define whether a system is in net erosional or depositional state (e.g., Catuneanu et al. 2009; Posamentier and Vail 1988; Shanley and McCabe 1994). If relative sea level falls at such rate that the coastal trajectory is exactly an extension of the equilibrium profile, progradation is not associated with aggradation along the longitudinal profile, which therefore can reach equilibrium (Helland-Hansen and Hampson 2009; Muto and Swenson 2005). More severe relative sea-level fall, such as associated with erosional unconformities and incised-valley systems, can lower the equilibrium profile to below the coastal-plain segment of the longitudinal profile, resulting in net erosion and efficient sediment transport from the hinterland to the river mouth. Conversely, during relative sea-level rise the conceptual equilibrium profile is raised, resulting in the creation of accommodation on the coastal plain. Subsequently, this results in reduced sediment transport to the shoreline and in thick coastal plain deposits.

In an upstream direction, the influence of relative sea-level variations is gradually reduced while controls such as water discharge, sediment supply, and tectonic regime increasingly influence sediment transport and the grade of systems (e.g., Catuneanu et al. 2009; Holbrook and Bhattacharya 2012; Posamentier and James 1993). Tectonic subsidence or uplift strongly determines long-term accommodation trends along the longitudinal profile (Miall 2013). Variations in water discharge and sediment discharge can alter the steepness of the equilibrium profile over relatively short time scales, resulting in alternating periods of aggradation and downcutting of fluvial systems that continuously develop towards new equilibrium profiles (Bijkerk et al. 2013; Holbrook et al. 2006; Simpson and Castelltort 2012). Fluvio-deltaic systems thus respond to the combined effect of upstream and downstream allogenic forcing mechanisms (e.g., Hampson et al. 2013), as well as inherent processes such as progradation, and tend towards a system-scale equilibrium state through continuous adjustments of the longitudinal profile. These adjustments shift sediment partitioning between the fluvial, deltaic, and marine environments of a sedimentary system and therefore determine the large-scale stratigraphic architecture.

The purpose of this contribution is to quantify how downstream external controls such as water depth in the receiving basin, eustatic sea-level variations, and subsidence rates affect the ability of a prograding fluvio-deltaic system to approach system-scale equilibrium, and how this affects sediment volume partitioning in fluvio-deltaic systems. This concept is examined through landscape models of fluvio-deltaic systems. We consider these models analogous to the coastal segment of fluvio-deltaic systems that supply sediment to shelf clinoforms into basins of up to a few hundreds of meters depth (Helland-Hansen et al. 2012), such as frequently found in foreland or rift basins as the Carboniferous Central Pennine Basin of northern England (Bijkerk 2014; Martinsen et al. 1995) or the Eocene Central Basin of Spitsbergen (e.g., Plink-Björklund and Steel 2006). Additional two-dimensional models are generated to examine the effect of progradation on the development of the longitudinal profile in terms of downstream fining. Subsequently, literature case studies of ancient small shelf clinoform systems are used to validate our findings.

3. METHODS

3.1 Experimental Facility

The results of four analogue models are described. The experimental setup consisted of a dual-basin configuration and allowed generation of two scenarios simultaneously: Model 1 (M1) and Model 2 (M2) (Fig. 2). Both models had a 1.6-m-wide rectangular duct serving as a fluvial zone that was connected to a subsiding basin that deepened away from the shoreline with discrete shallow, intermediate, and deep zones. Sediment and water entered the experiment diffusely through a pebble basket along the width of the fluvial duct. This setup allows the system to aggrade or degrade freely and does not enforce an upstream control on the elevation at which sand and water enter the experiment. Before an experiment, the longitudinal profile of each model was set to a downstream gradient of 0.01. The models had different subsidence scenarios, but they reached the same basin shape and depth at the end of the experiments (Fig. 3). Subsidence is generated with vertical adjustment of hexagonal blocks underneath the experimental set-up. Rows of these blocks are connected by overlying boards to generate smooth, rather than serrated, subsidence-zone boundaries (Fig. 2). An adjustable overflow controls the basinal water level during these experiments. All models are executed with fine quartz sand of a narrow grain-size distribution (D_{10} = 146 µm, D_{50} = 217 µm, and D_{90} = 310 µm).

In Experiment 1 - Model 1 (E1_M1), the effects of water depth are tested. Before starting this experiment, its basin was subsided to its final configuration. Therefore, this system experiences only a spatial increase in water depth as it progressively enters the shallow, intermediate, and deep zones of the experimental basin (Figs. 2, 3A). In Experiment 1 - Model 2 (E1_M2) the joint effects of subsidence and water depth are tested (Fig. 3A, B). During the first half of the experiment, the fluvio-deltaic system progrades over a non-subsiding substrate in shallow water, whilst during the second half the basinal area subsides at a rate of 2.5 mm h^{-1}. This results in subsidence-controlled accommodation on the delta plain, and both temporally and spatially increasing water depths (Figs. 2, 3B). In both E1_M1 and E1_M2 water discharge and sediment input were constant at 1 m^3h^{-1} and 0.004 m^3h^{-1}, respectively.

In Experiment 2, basinal water-level variations are also included to mimic eustatic sea-level variations, with different subsidence and discharge regimes for Model 1 (E2_M1) and Model 2 (E2_M2) (Fig. 3C, D; Table 1). Both models are affected by three asymmetric water-level cycles of 24 h period and variable amplitude. Cycle 1 starts with a 40 mm fall followed by a 30 mm rise. Cycle 2 has a 20 mm fall and rise, and cycle 3 has a 30 mm fall followed by a 40 mm rise, returning the water level to the initial level (Fig. 3C, D). In E2_M1, the subsidence rate is continuous throughout the experiment, resulting in the creation of accommodation on the delta plain and progradation into increasingly deeper water (Fig. 3C). Upstream, water discharge and sediment input were constant at 1.5 m^3h^{-1} and 0.004 m^3h^{-1}(Table 1). Water discharge is at a higher rate than in other models and theoretically leads to a faster equilibrium time and lower equilibrium gradient (e.g., Postma et al. 2008). In E2_M2, the entire basinal area is lowered 15 mm to accommodate water-level lowstand 1 (at 16 h) before the experiment starts. Subsidence at different rates for the shallow, intermediate, and deep zones starts after 24 h (Fig. 3D). In E2_M2 values are 1 m^3h^{-1} for water discharge and 0.004 m^3h^{-1} for sediment discharge, which is equal to the values in Experiment 1 (Table 1).

3.2 Experimental Procedure

The fluvio-deltaic systems were allowed to prograde during a start-up period prior to the actual experiment, so that experiments commenced with a natural, self-adjusted fluvial profile that reached the basin margin at 0 h (Fig. 2). Basinal water level during this period was 0 mm. Time-lapse photographs were taken at three-minute intervals to record the morphology of the fluvio-deltaic system.

The 96 h duration of E1_M1 and E1_M2 was subdivided into 12 intervals of 8 h (Table 1). Subsidence was applied to E1_M2 between these 12 intervals while the experiment was paused. Digital elevation models (DEMs) were measured with a laser scanner before and after subsidence to accurately constrain sediment budgets. The 72 h duration of E2_M1 and E2_M2 was similarly subdivided in 8 h intervals. Water level was adjusted at 20 min intervals.

3.3 Scaling

In the scaling of analogue models emphasis is placed on the stratigraphic similarity to real-world sedimentary systems, interpreting the large-scale stratigraphic patterns of such models as controlled miniature versions of such systems. In recent years, this type of experiment is increasingly recognized as a powerful tool in understanding the stratigraphic behavior of sedimentary systems in both space and time (e.g., Paola et al. 2009). The small size of these models allows rapid simulation of the stratigraphic architecture of real-world systems but does not incorporate properly scaled sedimentary processes and resultant facies.

The scaling relation between real-world landscapes and analogue experiments is based on characteristic length and time scales. Length scales (e.g., the length of the depositional segment of a river) are easily established, while time scales associated with stratigraphic development over such length scales are approached by non-linear diffusion equations (Paola et al. 1992a; Postma et al. 2008). Using an analogue scaling approach, landscape experiments can be set up to mimic the stratigraphic response of real-word systems to allogenic and autogenic controls. Landscape models have successfully reproduced stratal patterns that are commonly recognized in sequence-stratigraphic models such as incised valleys, sequence boundaries, maximum flooding surfaces, and system tracts (e.g., Koss et al. 1994; Martin et al. 2011; van Heijst et al. 2002; van Heijst and Postma

2001), while being able to determine the relative importance of controls (e.g., Kim and Paola 2007; Kim et al. 2006; Muto and Swenson 2006).

The style and record of responses of natural systems on forcing mechanisms depends on the ratio between time scales of forcing (T_{for}) and reactive time scales inherent to the system. For stratigraphic architecture, this reactive time scale has been termed the equilibrium time (T_{eq}) (Paola et al. 1992a). The ratio T_{for}/T_{eq} has proven to be effective for the simulation of stratigraphic response to various rates of relative sea-level variations (Bijkerk et al. 2013; Paola et al. 2009; Strong and Paola 2008; van Heijst and Postma 2001). Slow processes ($T_{for} >> T_{eq}$) are unable to drive a system away from equilibrium conditions because the system has sufficient time to adapt to new boundary conditions. Fast processes ($T_{for} << T_{eq}$) on the other hand, can strongly affect the grade of a fluvio-deltaic system because it is incapable of adapting at sufficiently fast rates to keep up with the forcing mechanism.

For well-constrained systems such as modern river systems and analogue models, diffusion equations can be used to describe sediment transport. The squared length of a fluvial system divided by its diffusivity provides an estimate of the equilibrium time (Paola et al. 1992a). Diffusivity is a function that is strongly dependent on water discharge per unit width and stream type. For braided systems it is approximated by a tenth of the width-averaged water discharge (Paola et al. 1992a). In E1_M1, E1_M2, and E2_M2 this results in an estimated equilibrium time of ~ 100 h at the start of the experiment. For E2_M1, the higher water discharge results in a higher diffusivity and thus in a shorter equilibrium time of ~ 72 h. The 24 h water-level cycles in Experiment 2 thus approximate a quarter (where T_{eq} = ~ 100 h) or third (where T_{eq} = ~ 72 h) of the estimated equilibrium time. Such ratios fall within the same range as many modern fluvial systems that are affected by 100 kyr eustatic sea-level cyclicity and have equilibrium times in the order of 100 – 1000 kyr (cf. Castelltort and Van Den Driessche 2003). The cyclic variations in the water level of Experiment 2 thus mimic high frequency sea-level variation relative to the equilibrium time of the fluvio-deltaic system that are best compared to the high-frequency, high-amplitude glacio-eustatic sea-level variations. Therefore, the water-level curve used is asymmetric with the duration of water-level fall twice as long as water-level rise as to mimic 100 kyr glacio-eustatic sea-level variations (e.g., Lisiecki and Raymo 2005).

The 20 – 40 mm water-level variations are representative of glacio-eustatic sea-level variations that typically range from 50 to 100 m. Therefore the 80 – 120 mm water depths in the intermediate and deep zones (Fig. 2) are analogous to water depths of up to several hundreds of meters. This implies that we are mimicking depositional systems that are typically defined as small shelf clinoforms (e.g., Helland-Hansen et al. 2012; Carvajal and Steel 2006; Plink- Björklund and Steel 2007; Steel et al. 2007). Because we mimic progradation of a small shelf clinoform, we have opted for a fluvial line source instead of a point source, because the latter would result in the construction of a fan-delta geometry (e.g., van Heijst and Postma 2001). The subsidence patterns represent variable tectonic scenarios in which subsidence increases away from the basin margin, and allow us to study their effect on the development of the longitudinal profile.

3.4 Dataset

Analyses are based on DEMs and supported by time-lapse images. DEM analyses are focused on the shape of the longitudinal profile and the percentage of sediment input that is transported past the shoreline during successive 8 h intervals.

The shape of the experimental longitudinal profiles is typically concave up. Laterally, both the concavity and the elevation of the longitudinal profile vary for each DEM (Fig. 4). To express the shape of the longitudinal profile a “fill percentage” and a “slope percentage” are calculated to express the concavity and the overall changes in gradient of the longitudinal profile, respectively (Fig. 4A). This method was chosen because a curve-fitting approach produced insufficiently accurate results and was therefore unsuitable to pick up minor variations in the shape of the longitudinal profile (e.g., Ohmori 1991; Rice and Church 2001; Snow and Slingerland 1987).

Along the width of the models, a series of imaginary right-angled triangles can be drawn between the top of the longitudinal profile, the roll-over point, and an upstream point at the same elevation as the roll-over point DEM (Fig. 4A). The “fill percentage” is defined as the volume percentage of these triangles that is below the actual sediment surface. A horizontal plane would represent 0% fill, while a linear sloping profile would represent a 100% fill of the longitudinal profile. Intermediate values provide a volumetric measure of the concavity of the longitudinal profile without focusing on the precise shape of such a profile (Fig. 4A).

In a similar way, the longitudinal profile can be expressed as a “slope percentage”, which can indicate temporal changes in the gradient of the longitudinal profile (Fig. 4A). This is here defined as the ratio between the sediment volume below the sediment surface and the volume below the estimated system-scale equilibrium gradient. In this case, a horizontal plane would represent 0% value while a 100% value would represent system-scale equilibrium conditions. The estimated system-scale equilibrium gradient is based on the gradient of the longitudinal profile of E2_M1 at 16 h, when the system achieved a nearly linear, steep slope, and 100% sediment bypass over a period of 8 h, implying conditions at or close to system-scale equilibrium.

The water discharge and the ratio of water discharge to sediment discharge in E2_M1 are higher than in the other experiments (Table 1), resulting in more efficient sediment transport at lower gradients. This also implies that the model has a lower equilibrium gradient compared to the other models (e.g., Postma et al. 2008). Because the estimation for the system-scale equilibrium gradient was derived from experiment E2_M1 at 16 h, a conversion is required to estimate the system-scale equilibrium gradient in the other models: E1_M1, E1_M2, and E2_M2. This conversion is based on the difference in longitudinal gradient between E2_M1 and E2_M2 at 0 h. At this time only water discharge differed while downstream parameters were equal. The 1.5 times higher water discharge in E2_M1 resulted in a 1.2 times shallower gradient, relative to E2_M2. Consequently, the system-scale equilibrium gradient in E1_M1, E1_M2, and E2_M2 is assumed at a 1.2 times steeper gradient than in E2_M1. This conversion is basic but yields results consistent with the expectations that the “slope percentage of the longitudinal profile” in the other models does not reach as high as in E2_M1. Still, comparison of the “slope percentage” of E2_M1 to other models depends on the validity of the above assumption.

Additionally, DEMs are used to calculate the ratio between sediment volume used for progradation and the total sediment volume, quantifying the efficiency of sediment transport to beyond the shoreline (Fig. 4B).

3.5 Grain-Size Experiments

Besides the four landscape experiments described above, Scenario 1 and Scenario 2 were run in a rectangular recirculation flume 0.48 m wide and 12 m long (Fig. 5). These models examine downstream sediment fining as a function of the ability of the fluvio-deltaic system to approach system-scale equilibrium. Quartz sand with a bimodal grain-size distribution was used with peaks at 216 µm and 420 µm (D_{50} = 285 µm). The coarse-grained tail with a diameter of > 1 mm (7% by weight) was used to assess downstream fining.

Water was recirculated to the upstream side of the flume, resulting in a constant water discharge of 5.5 m^3h^{-1} (Table 1; Fig. 5). The large width of the upstream weir functions to accelerate the slow-moving, large water column such that a thin water film enters the experiment at a constant velocity (Fig. 5). On top of this upstream weir, dry sediment was added through an overhead sediment feeder at a rate of 0.007 m^3h^{-1} (Table 1; Fig. 5).

Instead of starting with a natural, self-adjusted fluvial profile such as the previously described experiments, these experiments started as a 4 m horizontal plane. In this experiment, data recording starts while the system aggrades to its natural gradient. In Scenario 1, a downstream weir prevents progradation, allowing aggradation from horizontal plane up to the system-scale equilibrium gradient (cf. Muto and Swenson 2005; Postma et al. 2008). In Scenario 2, downstream of the horizontal plane, a basin of 3 cm water depth is present that allows shallow-water progradation.

Both Scenario 1 and 2 ran for 8 h (Table 1; Fig. 5). At half-hour intervals, five point measurements along the width of the flume at 0.25 m intervals were made to obtain a width-averaged longitudinal profile (Fig. 5B). In both experiments, grain-size samples of the final longitudinal profile were taken at 0.5 m intervals after the experiment finished. Additional grain-size samples were taken behind the downstream weir of Scenario 1.

Water discharge was chosen such that average water depth on the fluvial topset was sufficient to prevent preferential transport of coarse grains (cf. Vollmer and Kleinhans 2007). This resulted in the formation of current ripples but enabled assessment of the relation between downstream fining and longitudinal-profile development. The approximate equilibrium time at the start of these models is ~ 14 h, based on diffusion equations controlled by the length and width-averaged water discharge of this system (Paola et al. 1992a).

4. RESULTS

4.1 Experiment 1 - Basin 1 (E1_M1)

E1_M1 represents a pre-formed basin with constant water level and results in progradation of a shelf clinoform system into a spatially deepening basin (Fig. 6A – C; Fig. 8A, B). The fill percentage of the longitudinal profile increases from 91% to ~ 96% from 1 to 56 h and subsequently decreases to 94% (Fig. 6G), indicating that the concavity initially decreases before increasing again (Fig. 4A). The slope percentage of the longitudinal profile starts at 76% and increases to 92% from 1 to 56 h, indicating that the longitudinal gradient steepens, after which it remains constant (Fig. 4A; Fig. 6H). These trends correlate well with the sediment bypass pattern, which starts at ~ 24% of the sediment input volume and increases towards a maximum of 50% from 56 to 64 h, implying that increasing sediment volume is transported to beyond the shoreline. Subsequently, it decreases to ~ 43% (Fig. 4B; Fig. 6F).

Over the duration of the experiment, the average clinoform height, measured along the strike of the clinoform, gradually increases from 25 to 96 mm during the experiment and correlates with the sediment bypass percentage and the fill and slope percentages (Fig. 6C, F – H). The progradation rate decreases from 14 to 9 mm h^{-1} (Fig. 6E) and results in a gradual increase in the size of the longitudinal profile from 2.6 to 6.1 m^2 (Fig. 6D).

4.2 Experiment 1 - Basin 2 (E1_M2)

E1_M2 initially forms in a shallow ramp-style basin with constant water level that from 48 h onwards subsides at a rate of 2.5 mm h^{-1} (Fig. 7A, B). Shallow-water conditions allow rapid progradation during the first half of the experiment. During the second half, tectonic subsidence results in accommodation on the topset and in a deepening of the basin, which reduces the progradation rate (Fig. 7C – E; Fig. 8 C, D). At the start of the experiment, sediment bypass is 5% of the sediment input and increases to ~ 16% at 40 – 48 h (Fig. 7F). The initiation of subsidence reduces sediment bypass to 8% (Fig. 7F, 48 – 56 h), after which it steadily increases to 24% at the end of the experiment (Fig. 7F, 88 – 96 h). The fill percentage of the longitudinal profile starts at 86% and increases rapidly towards 92% at 64 h (i.e., becomes less concave; Fig. 4A), at which point it becomes approximately constant (Fig. 7G). The slope percentage of E1_M2 initially remains low at 74% (i.e., progrades at a low gradient) and gradually increases to 87% after the initiation of subsidence, implying that the gradient becomes steeper (Fig. 7E, H; Fig 4A).

Sediment bypass is low in the rapidly prograding system and coincides with a strongly concave, low-gradient longitudinal profile (Fig. 7E – H, 0 – 48 h). After 48 h, the basin subsides rapidly and a significant sediment volume is captured for topset aggradation, decreasing the sediment bypass rate (Fig. 7E – H, 48 – 72h; Fig. 8C, D). Notably, towards the end of the experiment this sediment bypass rate increases to its highest levels (Fig. 7C, E, F, 72 – 96 h). This coincides with slow deep-water progradation and corresponds to an increasing fill and slope percentage of the longitudinal profile (Fig. 7E – H), indicating a decreased concavity and an increased longitudinal gradient compared to earlier parts of this experiment (Fig. 4A).

4.3 Experiment 2 - Basin 1 (E2_M1)

Throughout this experiment, subsidence is continuous and the water level in the receiving basin mimics three glacio-eustatic cycles of constant frequency and variable amplitude (Fig. 9A). This results in three regression – transgression cycles (Fig. 8E, F) that are reflected in the cyclicity of the measured parameters (Fig. 9C – H).

The style of deposition and erosion changes significantly during a mimicked sea-level cycle and varies between cycles as well (Fig. 11; Fig. 12). During normal regression, the entire fluvio-deltaic topset is frequently active (Fig. 11A). During forced regression, two modes occur: small parts of the topset become inactive, generating short-lived interfluves in cycles 1 and 2 and the start of 3 (Fig. 11B). During relative sea-level fall 3, an incised valley forms that focuses much of the water and sediment discharge along a narrow section of the delta topset, generating long-lived interfluves (Fig. 11C). This leads to significant progradation focused at the deep-water segment of the basin, after which the valley mouth shifts towards the shallower segment at a later stage (Fig. 11D). During transgression, small lobes step back onto the lowstand shelf while in an upstream direction discharge is still focused in the incised valley (Fig. 11E).

The fill and slope percentages, proxies for concavity and gradient of the longitudinal profile (Fig. 4A; Fig. 9G, H), as well as sediment bypass beyond the shoreline, show close correspondence to the relative sea-level variations (Fig. 9B, F). The highest bypass rates are observed during late sea-level fall and lowstand and coincide with increasing fill and slope percentages of the longitudinal profile (i.e., longitudinal profiles become less concave and steeper; Fig. 9F – H, 8 – 16 h, 32 – 40 h, 56 – 64 h). Low sediment bypass occurs during the sea-level rise and coincides with a decreasing fill and slope percentage of the longitudinal profile (i.e., longitudinal profiles become more concave and less steep; Fig. 9F – H, 16 – 24 h, 40 – 48 h, 64 – 72 h). Intermediate rates for sediment bypass, fill percentage, and slope percentage of the longitudinal profile occur during sea-level highstand and early sea-level fall (Fig. 9F – H, 0 – 8 h, 24 – 32 h, 48 – 56 h).

During late relative sea-level fall in cycles 1, 2, and 3 the sediment bypass rate is 102, 63, and 126% of the sediment input, respectively (Fig. 9F). Sea-level fall 3 is smaller than sea-level fall 1 (30 vs. 40 mm) but results in incised-valley formation and significantly higher sediment bypass (Fig. 9F). Valley incision coincides with an increased water depth in the receiving basin and an increased fill percentage of the longitudinal profile, indicating a decreased concavity (cf. Fig, 9C, G, 8 – 16 h and 56 – 64 h). Interestingly, it also coincides with a reduced slope percentage relative to the first sea-level fall (cf. Fig. 9H, 16 h and 64 h), indicating that erosion within the incised valley occurs at a lower gradient than during sea-level fall 1.

Erosion-deposition maps also show that during relative sea-level fall 3 significantly more erosion occurs on the delta topset than during relative sea-level fall 1 (Fig. 12A, C). In the case of relative sea-level fall 3, erosion migrates upstream and results in significant erosion that persists until the end of the subsequent relative sea-level rise (Fig. 12D).

4.4 Experiment 2 - Basin 2 (E2_M2)

The input parameters of E2_M2 differ from E2_M1 in two ways. Firstly, water discharge is 1 m^3h^{-1} instead of 1.5 m^3h^{-1} (Table 1). Secondly, the system progrades on a shallow, non-subsiding ramp during sea-level fall 1, resulting in the very shallow-water conditions at lowstand 1 (Fig. 10A, B, 8 – 16 h).

Sediment bypass shows a similar response to relative sea-level variation as in E2_M1 but bypasses a smaller percentage of the sediment beyond the shoreline. The fill percentage of the longitudinal profiles is lower, indicating that these profiles are more concave (cf. Fig. 9G and 10G). A second difference is that the fill and slope percentages of the longitudinal profile decrease during sea-level fall to lowstand at 16 h, whereas in E2_M1 these values increase (cf. Fig. 10G, H and Fig. 9G, H, 16 h). This difference coincides with very high progradation rates and shallow water depth of < 5 mm in the basin (Fig. 10C, E, 8 – 16 h).

4.5 Grain-Size Experiments

Scenarios 1 and 2 indicate that the development of the longitudinal profile and the grain-size distribution along this profile are dependent on the progradation rate (Fig. 13). In Scenario 1 a weir obstructed progradation, which resulted in the gradual development of an increasingly steeper longitudinal profile (Fig. 13A). Towards the end of the experiment successive profiles overlap along a steep and nearly linear longitudinal profile, indicating that the profile did not aggrade significantly after 5.5 h (Fig. 13A). Grain-size data collected below the downstream weir (Fig. 5) indicate that after 4.5 h the coarse-grained fraction bypassed the weir approximately at the same ratio as the input ratio, indicating that downstream fining was no longer efficient (Fig. 13C). This is further supported by samples along the final longitudinal profile that do not indicate a downstream-fining trend (Fig. 13B).

In Scenario 2, the fluvio-deltaic system prograded into shallow water, lengthening the longitudinal profile from 4 to 5.5 m. Initially, the system aggrades a wedge on the horizontal plane while it becomes progradational from 4 h onwards, indicating that it has reached a natural gradient along the length of the initial horizontal plane. Compared to Scenario 1, the longitudinal profile of Scenario 2 remains more concave and maintains a substantially lower longitudinal gradient ([1:107] vs. [1:180]), while sediment and water discharge were the same in both experiments (cf. Fig. 13A and 13D; Table 1). Grain-size data collected along the final longitudinal profile in Scenario 2 shows that coarse-grained sand is preferentially retained in the relatively steep, upper reach of the profile

(Fig. 13E). The lower reaches are relatively finer grained, indicating that this progradational system effectively becomes finer downstream.

5. CONTROLS ON FLUVIAL PROFILE SHAPE AND FLUVIO-MARINE SEDIMENT PARTITIONING

5.1 Water Depth in the Receiving Basin

With constant relative sea level, prograding systems cannot achieve system-scale equilibrium (e.g., Fig. 6F, H; Fig 13D; Fig. 14A – D; Muto and Swenson 2005), due to aggradation along the longitudinal profile. In shallow-water conditions, such as occur at the start of E1_M1, E1_M2, and in Scenario 2, fluvio-deltaic systems require limited sediment volumes deposited beyond the shoreline to prograde rapidly. This results in strongly concave profiles at significantly lower gradients than the equilibrium gradient, as indicated by a low fill and slope percentage of the longitudinal profile (e.g., Fig. 6G, H; Fig. 7G, H, 0 – 48 h; Fig. 14B). Such systems transport sediment inefficiently and deposit the bulk of their sediment load along the fluvio-deltaic topset (e.g., Fig. 7F, 0 – 48 h). The progradation rates of fluvio-deltaic systems prograding into deep water are significantly lower and allow the longitudinal profile to aggrade to a less concave and steeper gradient (i.e., approach the equilibrium gradient; e.g., Fig. 6E, H, 48 – 96 h). Such systems transport sediment more efficiently along the fluvio-deltaic topset and partition a significantly larger percentage of their sediment load beyond the shoreline, where it becomes available for further redistribution in the marine domain (Fig. 6F, 48 – 96 h; Fig. 14C).

Progradation will gradually slow down in fluvio-deltaic systems that build a shelf clinoform into a spatially deepening water body, such as ramp-style basin margins (e.g., Fig. 6C, E). A reduction in the progradation rate allows the longitudinal profile to become steeper and less concave (Fig. 6G, H; Fig. 14D), which increases the efficiency of sediment transport and enhances sediment transport to beyond the shoreline (Fig. 6F; Fig. 14D). Therefore, a shift in the longitudinal sediment partitioning can be expected in systems where the water depth (i.e., shelf clinoform height) increases spatially, over time depositing a smaller percentage of the sediment load in the fluvial and delta-top systems and more in the progradational delta-front and slope clinoform successions (Fig. 6F; Fig. 14D). This process provides a potential mitigation mechanism for autoretreat (Muto 2001; Muto and Steel 2002b) that is further discussed in the autostratigraphy section.

Downstream sediment fining occurs in both gravel- and sand-bed rivers and is dependent mainly on selective transport, although in gravel-bed rivers abrasion processes are important as well (Frings 2008; Paola et al. 1992b). Selective transport is ineffective in longitudinal profiles that are in system-scale equilibrium: fine-grained sand is more quickly transported than coarse-grained sand but the latter will arrive as well, removing the downstream-fining trend (Fig. 13A - C; Fig. 14A). However, if a profile is below system-scale equilibrium, selective transport can result in stable downstream-fining trends (Fig. 13D, E; Fig. 14B, C) as a result of downstream decreases in bed shear stress (Knighton 1999; Rice and Church 2001) or a downstream decrease in capacity to transport the coarse grains by suspension transport (Frings 2008). In Scenario 1, a nearly linear longitudinal profile develops after ~ 5.5 h. Longitudinal profiles at successive time steps overlap this profile, implying that the system has aggraded to an approximate equilibrium gradient (Fig. 13A; Fig. 14A). This approximately coincides with the arrival of coarse-grained sediment at the downstream weir in similar quantities to those in sediment input (Fig. 13C). Downstream fining has thus become ineffective, which is further confirmed by the grain-size distribution along the final longitudinal profile (Fig. 13B; Fig. 14A).

In Scenario 2, a progradational system developed with a low-gradient, concave profile (Fig. 13D; Fig. 14B). Here, coarse-grained sand is retained in the steep upper reach of the fluvial profile, indicating that the transport capacity at lower gradients is insufficient to transport the coarse sediment fraction. Abrasion processes are insignificant in these models, and the difference between both experiments suggests that the downstream-fining rate correlates with the concavity and gradient of the longitudinal profile (e.g., Wright and Parker 2005a, 2005b), which in turn depend on progradation of the shoreline. The rate of progradation depends strongly on the water depth of the receiving basin (e.g., Fig. 6; Fig. 7; Fig. 14B, C), which thus influences the depositional character in the fluvial to marine domain and forms a downstream allogenic control on both the volume and the grain size of available sediment that can potentially be remobilized and distributed into deeper marine environments (Fig. 14B – D).

5.2 Subsidence

E1_M2 examines the effects of water depth and subsidence. Shallow-water progradation on a non-subsiding substrate during the first half of the experiment allows high progradation rates in comparison to E1_M1 (cf. Fig. 7C, E and Fig. 6C, E). This results in a concave, low-gradient longitudinal profile (Fig. 7G, H) and results in low sediment volumes bypassing the shoreline (Fig. 7F; Fig. 14B). The initiation of subsidence in the basin from 48 h onwards increases the water depth at the shelf edge while generating substantial accommodation along the longitudinal profile, impeding rapid progradation and maintaining low sediment bypass rates (Fig. 7). The reduced progradation rate triggers a continuous increase in the gradient and a decrease in the concavity of the longitudinal profile (Fig. 4A; Fig. 7G, H). From 80 h onwards, the sediment bypass volume beyond the shelf edge increases to a higher level than that in the shallow non-subsiding basin, even though the high subsidence rate is maintained (Fig. 7B, F). Subsidence therefore has two counteracting effects: subsidence upstream of the shoreline generates accommodation and requires additional sedimentation and potentially increases the concavity of the longitudinal profile (Sinha and Parker 1996). However, it also reduces the progradation rate by increased deposition on the topset and by an increase in clinoform height, allowing the fluvio-deltaic system to more closely approach equilibrium. In this experiment, progradation across a rapidly subsiding fluvio-deltaic topset (from 48 h onwards) was more efficient in bypassing sediment beyond the shelf edge than the shallow-water system on a non-subsiding substrate (from 0 – 48 h) (Fig. 7F; Fig. 8C, D; Fig. 14D).

5.3 Sea Level

In E2_M1, basinal water-level variations are used to mimic glacio-eustatic sea-level variations. These variations influence sedimentation in a basin that subsides at a constant rate (Fig. 9A, B), resulting in the progradation of a shelf clinoform in increasing water depths (e.g., Fig. 8E, F). High-frequency sea-level variations form a strong additional control on the grade of the longitudinal profile (e.g., Blum and Hattier-Womack 2009). As a first-order approximation, a sequence-stratigraphic interpretation based on relative sea-level variations alone provides a good explanation for the stratigraphic stacking pattern (Fig. 8E, F). During sea-level rise, the downstream reaches of the fluvio-deltaic system are aggradational and step back on the lowstand shelf (Fig. 11E). Sea-level rise predominantly raises the lower reach of the longitudinal profile, resulting in a strongly concave profile, shifted away from the system-scale equilibrium gradient (Fig. 9G, H; Fig. 14H). During relative sea-level fall, the lower reaches of the longitudinal profile are eroded while deposition continues upstream of sea-level influences (e.g., Fig. 12A). This generates a nearly linear profile that is close to the system-scale equilibrium gradient (Fig. 9G, H; Muto and Swenson 2005) and results in efficient sediment transport to the coastline (Fig. 9F; Fig. 14E, F). However, a relative sea-level-based sequence-stratigraphic solution cannot explain why an incised valley formed only during the moderate sea-level fall 3 (30 mm, Fig. 12C, 48 – 64 h), and not during the larger sea-level fall 1 (40 mm, Fig. 12A, 0 – 16 h).

Low shoreline progradation rates, in these experiments associated with deep-water conditions, lead to steeply descending shoreline trajectories during sea-level fall (Helland-Hansen and Hampson 2009), steepening the longitudinal profile. Additionally, systems prograding into deep water approach equilibrium conditions relatively closely compared to systems with higher progradation rates (Fig. 6; Fig. 7). Combined, this allows systems to become strongly erosional locally (Fig. 11; Fig. 12; Fig. 14G), a prerequisite for the initiation of coastal incised valleys (Strong and Paola 2008). After valley incision, nearly all discharge is funneled through the incised valley. This causes an increase in the water discharge per unit width, lowering the gradient at which the incised-valley system is in equilibrium (cf. Fig. 9H, 16 and 64 h), thereby triggering increased and prolonged erosion (Fig. 9F; Fig. 14G). The latter is observed during sea-level fall 3, during which erosion migrates upstream within a valley and persists until the following sea-level highstand (Fig. 12D). In this situation, erosion has thus decoupled from sea-level fall and is maintained by the lowering of the fluvial gradient within the incised valley, allowing an increased diachroneity of the sequence boundary (cf. Fig. 12B and Fig. 12D; Strong and Paola 2008).

A sea-level fall of similar amplitude in shallow-water systems will result in a more gradual descending shoreline trajectory due to a higher progradation rate of the shoreline, causing the longitudinal gradient to be further removed from system-scale equilibrium (Helland-Hansen and Hampson 2009). Therefore, the rate of sea-level fall needs to be much more dramatic to steepen the longitudinal profile sufficiently to surpass the equilibrium profile and trigger incision. Substantial incision is thus less likely in shallow-water systems, hindering the formation of incised-valley systems. If progradation rates are sufficiently high, systems might even remain aggradational during relative sea-level fall. In E2_M2, for example, rapid progradation due to the exceptionally shallow-water conditions during sea-level fall 1 forces the fluvio-deltaic system away from equilibrium conditions, while in other occurrences equilibrium is approached during sea-level fall (cf. Fig. 9 and Fig. 10). Such a scenario might occur in shallow-water systems or on wide shelves before sea level falls below shelf edge. In such cases, the reduction of the longitudinal gradient might result in aggradation rather than incision of the fluvio-deltaic succession even during sea-level fall (Ethridge et al. 1998; Petter and Muto 2008; Prince and Burgess 2013; Swenson and Muto 2007; Wallinga et al. 2004). Water depth thus strongly modulates the sensitivity of the fluvio-deltaic system to erosion induced by sea-level fall and to the formation of incised valleys.

The incised valley of E2_M1 began in the deep zone of the experimental basin (Fig. 2; Fig. 11C), and we speculate that this is the most likely position, rather than lateral positions in the shallow to intermediate depth zones. In depositional environments with lateral differences in water depth, the deep segments will require longer time spans of fluvial activity to infill due to the larger sediment volumes required. Additionally, the avulsion frequency of channels feeding such segments might be reduced because avulsion frequency appears to be partially controlled by the lengthening of the distributary channels (Edmonds et al. 2009), which will be slower due to lower progradation rates. Therefore, it is likely that channels are present at positions feeding into the deepest segments for prolonged periods, enhancing the probability of incision at such locations. Such control on the lateral position of incised valleys within a depositional system is thought to be relevant mainly when large lateral variations in water depth occur along short distances such as rift basins.

5.4 Ratio of Water Discharge to Sediment Discharge

An increased water-to-sediment ratio results in more efficient sediment transport at lower gradients (e.g., Simpson and Castelltort 2012), and can affect incised-valley formation and style (Bijkerk et al. 2013). This is also indicated by the differences between E2_M1 and E2_M2 (Fig. 8; Fig. 9; Fig. 10). The water-to-sediment ratio is 1.5 times higher in E2_M1 than in E2_M2. This resulted in an ~ 1.2 times lower longitudinal gradient (see Section 3.4, Dataset) and between 1 to 1.5 times higher sediment bypass rates during sea-level fall (cf. Fig. 9F and Fig. 10F), implying significantly more voluminous deposition in the delta front (cf. Fig. 8E, F and Fig. 8G, H). Additionally, higher water discharge per unit width such as occurs in E2_M1 relative to E2_M2 results in shorter equilibrium times (see Section 3.3; Paola et al. 1992a), implying that a system will adapt more rapidly to changing conditions such as relative sea-level fall. In E2_M1, these more favorable upstream parameters resulted in lower concavity of the longitudinal profile and incised-valley formation when the experimental basin reached a sufficient depth during sea-level fall 3 (cf. Fig. 9G, H; Fig. 10G, H). In E2_M2, the longitudinal profile remained significantly more concave, resulting in lower sediment transport rates to the coastline and more deposition on the topset (Fig. 10F, G).

5.5 Autostratigraphy

Autostratigraphic principles (Muto et al. 2007) state that sedimentary systems influenced by constant discharge and a constant rate of relative sea-level rise may transition from initial normal regression, where sediment supply is still in excess of the accommodation creation, into transgression or “autoretreat”. This is due to the increasing budget required to aggrade both slope and topset of the sedimentary system (Muto 2001). At the autoretreat break, the increasing size of the system reaches a tipping point at which sediment supply cannot support further progradation, and 100% of the sediment load is partitioned to the topset. A subsequent increase in the topset area due to landward onlap can cause the system to autoretreat (Muto and Steel 2002a).

The present results reveal an autoretreat mitigation mechanism. Progradation during relative sea-level rise implies that the system builds out into increasing water depths, resulting in a slowing of the progradation rate. The results suggest that this leads to an increase in the longitudinal gradient and a reduction of its concavity (i.e., an increase in both the fill and slope percentage; Fig. 6; Fig. 7), causing increasing rates of sediment bypass to beyond the shoreline. This enhanced sediment transport efficiency increases the sediment volume available for progradation of the fluvio-deltaic system, while it decreases the sediment volume that is used to for aggradation along the longitudinal profile. This mechanism of increasing sediment bypass rates during progradation into increasing water depths is well illustrated in E1_M1 and E1_M2.

In E1_M1, the partitioning of sediment to beyond the shoreline doubles during progradation into a basin of increasing water depth (Fig. 6C, F), despite a twofold increase in topset area (Fig. 6D) (note that relative sea level is static and the water-depth increase refers to a spatial increase). In E1_M2, from 0 - 48 h, a low-gradient, strongly concave longitudinal system develops on a non-subsiding substrate. Subsequently, a constant subsidence rate from 48 h onwards initially slows the progradation rate due to the increase in accommodation along the longitudinal profile, and due to the increasing water depth at the shelf edge (Fig. 7). This leads to a steepening of the longitudinal gradient and a decrease in its concavity, which in turn results in increasing fluvial efficiency and increasing sediment bypass towards the end of the experiment (Fig. 7). Whilst not excluding the possibility of autoretreat, these results indicate that enhanced fluvial efficiency in routing sediment beyond the shoreline as a consequence of increasing water depth may counter or delay its occurrence.

From 56 h onwards, both the gradient and the concavity of the E1_M1 longitudinal profile remain constant (Fig. 6G, H), suggesting that the system has reached a balance between its approach towards system-scale equilibrium conditions and the corresponding progradation related to the high rates of sediment bypass to the shoreline. The constant gradient and concavity imply that the increasing topset area (Fig. 6D) requires greater amounts of sediment, as is reflected in the slow decrease in the sediment-bypass percentage (Fig. 6F). This suggests that when such a balanced state is attained, autostratigraphic principles might apply in a straightforward manner.

6. APPLICATION

The coupling of the concept of system-scale equilibrium to shoreline progradation has been used to explain that equilibrium on geologically relevant time scales can be obtained only during relative sea-level fall, suggesting that sedimentary systems are generally not in equilibrium (Muto and Swenson 2005). The current analogue-model dataset indicates that non-equilibrium results in a broad spectrum of sediment partitioning trends along the longitudinal profile that might result in variable stratigraphic patterns that are not related to allogenic forcing mechanisms, and becomes predictable when related to water depth in the receiving basin.

Accommodation in fluvial settings is defined as the volume between the longitudinal profile and the conceptual equilibrium profile (Posamentier and Allen 1999), and is closely related to longitudinal patterns of sediment partitioning. The current results indicate that accommodation is generally present in progradational systems without relative sea-level fluctuations, but that the infill of such space becomes increasingly difficult when approaching the equilibrium profile (e.g., Fig. 6;

Fig. 13; Postma et al. 2008). Therefore, in slowly prograding systems that are close to equilibrium, low rates of topset aggradation and high rates of sediment bypass beyond the shoreline can be expected whereas in rapidly prograding systems the opposite occurs. In fluvial outcrops, such different scenarios would be observed as either low- or high-accommodation-style fluvial deposits, although tectonic subsidence trends might be a more prominent cause. Gradual changes between such low- or high-accommodation states are potentially related to changing water depth and do not necessarily relate to relative sea-level variations or variable subsidence rates in the fluvial domain.

In the deltaic domain, the arrival of increasing volumes and grain sizes might be coupled to the arrival of the shelf edge in deep water, where it can trigger increasing activity of linked turbidite systems (e.g., Nelson et al. 2009). Therefore, knowledge of water depth and associated progradation rates might help interpret and predict stratigraphic trends in both the fluvial, deltaic, and marine domains.

Based on these experiments, stratigraphic trends related to the efficiency of sediment transport along the longitudinal profile are likely present in shelf clinoforms. The importance of such trends in natural systems relative to other upstream factors such as changes in the sediment discharge or water discharge, for example due to tectonic or climate regime, or downstream controls such as relative sea level, has yet to be determined. Effects might be obscured if small or misinterpreted if significant. Additional work on shelf clinoform successions will be required to determine the relative importance in different settings. Based on literature review two case studies of shelf-margin successions are selected that demonstrate aspects of these analogue models in natural systems. Both case studies, the Maastrichtian Lance - Fox Hills - Lewis shelf margin of southern Wyoming and the Eocene Central Basin of Spitsbergen have relatively small, mountainous catchment areas and prograde for several tens of kilometers into basins with water depths of several hundreds of meters. Such small sedimentary systems respond relatively quickly, making it more likely that the variations in the grade of the longitudinal profile are recorded recognizably in the stratigraphic record.

6.1 Case study 1: The Maastrichtian Lance - Fox Hills - Lewis shelf margin, Southern Wyoming

The Maastrichtian Lance - Fox Hills - Lewis shelf margin of southern Wyoming is a well-studied shelf-margin succession that can be used to test the concepts from analogue modeling in a setting that is not influenced by high-amplitude, high-frequency glacio-eustatic variation (e.g., Miller et al. 2005; Carvajal 2007), analogous to Experiment 1 in this study.

Over a period of 1 to 1.5 Myr, rapid shelf-margin accretion resulted in the formation of 15 clinothems (Carvajal 2007; Carvajal and Steel 2006, 2009, 2012) that can be subdivided into two stages. The first stage was deposited in a rapidly subsiding basin and is represented by clinothems C0-C9 (Fig. 15A). Based on the gradually but irregularly rising shelf-edge trajectory, an overall water depth increase from ~ 250 to > 400 m is recorded. Subsidence was directly linked to Laramide tectonic activity across the region, triggering subsidence in the basin and uplift in its source area (Carvajal 2007; Carvajal and Steel 2012). Stage 2, represented by clinothems C10-15, began when active thrusting and uplift in the source area had decreased or ceased (Carvajal 2007). These clinothems form a progradational succession in a basin of fairly constant depth, as reflected by the low-angle to horizontal shelf-edge trajectory (Fig. 15A; Carvajal and Steel 2006).

The average sediment supply rate calculated for Stage 1 is ~ $4 – 10 * 10^6$ ton / yr; the progradational succession of Stage 2 has a higher sediment supply rate of $8 – 16 * 10^6$ ton / yr during a period of tectonic inactivity (Carvajal 2007, Carvajal and Steel 2012). The increase in sediment supply from Stage 1 to Stage 2 is counterintuitive since the decreasing rate of thrusting in the source area is expected to correspond to a decrease in the sediment yield. The increase in sediment yield is therefore linked to modest uplift due to isostatic rebound, persistence of high relief, and increasing catchment area (Carvajal 2007; Carvajal and Steel 2012). Additionally, the overall sand/shale ratio increases over time, which has been ascribed to erosion of increasingly sandy source rock, documented from the stratigraphy of the region (Fig. 15B; Carvajal 2007, Carvajal and Steel 2012).

We suggest, as an additional hypothesis that the progressive increase in water depth during Stage 1 and the near-cessation of relative sea-level rise at the transition from Stage 1 to Stage 2 can contribute to the increase in sediment volume and the increase in sand/shale ratio. The sea-level stillstand and increased water depth allow the longitudinal profile to grade closer towards equilibrium (Fig. 15C). This enhances the sediment bypass rate and allows transport of coarser sediment into the basin, which increases the sand/shale ratio in both the basin floor and overall (Fig. 15B).

6.2 Case study 2: Eocene Central Basin, Spitsbergen

The Eocene Central Basin of Spitsbergen provides one of very few outcrops of well-preserved shelf-margin clinothem complexes, from coastal plains to deepwater fans. Sea-level cyclicity is estimated at ~ 300 kyr duration (Crabaugh and Steel 2004). Two contrasting shelf-margin types, Types I and II, developed broadly at the same period within the region (Plink-Björklund and Steel 2005) and demonstrate the influence of basin depth and progradation rate on incised-valley formation.

Type I shelf margins are characterized by severe erosion of the outer shelf by falling-stage shelf-edge deltas, accompanied by the formation of significant basin-floor fans that are fed from across a disrupted slope (Plink-Björklund and Steel 2005). Shelf-margin accretion occurs mainly during the late lowstand and occurs in water depths of 300 – 350 m (Plink-Björklund and Steel 2005; Steel et al. 2007). Type II shelf margins are characterized by the absence of a basin-floor fan and accrete with an amalgamated succession of falling-stage, early, and late lowstand deltas. Falling-stage deltas are notably highly progradational. Of Type II margins, only the Reindalen clinothems (26-27) show complete exposures including the clinothem top. In these clinothems, water depth is estimated at ~ 200 m (Plink-Björklund and Steel 2002, 2005, 2007).

Both clinothem types are broadly coeval, and eustatic sea level is interpreted to fall below the shelf edge in both shelf-margin styles (Plink-Björklund and Steel 2005). Therefore, the different character is dependent on other inherent characteristics of these shelf types. Plink-Björklund and Steel (2005) suggest that a higher ratio of sediment discharge to water discharge and higher rates of sediment fallout at the shelf edge and upper slope during the falling stage in Type II shelf margins damps incision and prevents deep channeling at the shelf edge. Alternatively, the shallow water depth of Type II clinothems facilitates higher progradation rates, impeding incision due to the resultant lower gradient of the descending shoreline trajectory (cf. Fig. 7E, F, 0 – 16 h; Fig. 14E; Holbrook et al. 2006). Type I clinothems formed in deeper basins and are characterized by slower progradation rates, resulting in a slightly steeper downward-directed shoreline trajectory with the same rate of sea-level fall. This causes the longitudinal profile to become above grade and allows sufficient shelf incision to generate incised feeder channels (cf. Fig. 7E, F, 48 – 64 h; Fig. 14G; Strong and Paola 2008). Consequently, the likelihood of shelf incision during sea-level fall increases with water depth in the receiving basin, resulting in the different development of Type I and Type II deltas. Dependent on the water depth, both the timing of shelf-margin progradation differs and the gross architecture of shelf clinoform is altered.

7. CONCLUSIONS

Analogue modeling is used to examine the impact of basinal water depth and downstream allogenic controls on the temporal development of the longitudinal profile of progradational fluvio-deltaic systems and associated small-scale shelf margins. Analyses focus on the relationship between the gradient and concavity of the longitudinal profile and the corresponding sediment transport efficiency. System-scale equilibrium is defined as an end member and represents a state in which the longitudinal profile does not change shape while all sediment is bypassed beyond the shoreline. With constant relative sea level, progradational fluvio-deltaic systems develop towards but cannot reach this state because lengthening of the longitudinal profile requires continuous aggradation along the longitudinal profile. This implies that the departure from system-scale equilibrium is governed by the progradation rate. Water depth, subsidence, and sea-level variations act as allogenic controls on the migration of the shoreline, thus affecting how closely the fluvio-deltaic profile approaches equilibrium, thereby controlling the development of the longitudinal profile and fluvial to marine sediment partitioning.

Shallow water depth results in rapid lengthening of the sedimentary system. This causes a strongly concave, low-gradient longitudinal profile that is associated with high aggradation rates in the fluvial domain and strong downstream-fining trend. In deep-water systems, shoreline progradation rates are significantly lower, allowing the longitudinal profile of sedimentary systems to steepen and approach equilibrium more closely. This results in limited accommodation in the fluvial domain and high sediment supply to the shoreline with limited downstream fining. Increasing water depths, for example in ramp-style basins, reduce the progradation rate and therefore gradually shift the partitioning of sediment from mainly fluvial towards predominantly marine deposition. Water depth, through its effect on progradation rates, thus influences the sediment partitioning of sedimentary systems and forms a first-order control on the availability of sand-rich sediments that can potentially be remobilized and redistributed into deeper marine environments.

Subsidence has a dual effect: it generates accommodation along the longitudinal profile, limiting sediment transport to the shoreline. Counterintuitively, the resultant slow progradation rates can allow the fluvio-deltaic system to grade towards equilibrium, which can eventually increase the sediment transport efficiency along the longitudinal profile.

Relative sea-level variations rapidly alter the fluvio-deltaic longitudinal gradient. In deep-water systems, low shoreline progradation rates result in steeply descending shoreline trajectories during relative sea-level fall, generating significantly greater erosion than in shallow-water systems. Deep-water conditions therefore result in higher sediment yields beyond the shoreline and an increased probability of incised-valley formation. The latter can alter the timing of shelf-margin progradation and its gross morphology and therefore affect the transfer of sediment to deep marine sinks. The experimental results indicate that, during glacio-eustatic sea-level cyclicity, the longitudinal profile is closest to equilibrium during relative sea-level fall and early lowstand. This results in efficient sediment transport towards the shoreline, explaining delivery of increased sediment volumes of increasing grain size to lowstand systems tracts as a parameter controlled by relative sea level and water depth.

8. ACKNOWLEDGEMENTS

This work is in part funded by a British Geological Survey University Funding Initiative PhD studentship (BUFI S194) to J.B., sponsors of the Turbidites Research Group, and the University of Leeds. We are grateful to Thony van Gon Netscher, Henk van der Meer, and Dineke Wiersma for support during the experiments. We thank Michael Ellis and Oliver Wakefield for their comments on an earlier version of the manuscript. Suggestions from reviewers Ron Steel, Jacob Covault, Cristian Carvajal, and JSR editor Tobi Payenberg greatly improved the manuscript. J.B. and C.N.W. publish with the permission of the Executive Director, British Geological Survey, Natural Environment Research Council.

9. REFERENCES

Bijkerk, J.F., 2014, External Controls on Sedimentary Sequences: A Field and Analogue Modelling Based Study [unpublished PhD thesis]: University of Leeds, Leeds, 259 p.

Bijkerk, J.F., Postma, G., Ten Veen, J., Mikes, D., Van Strien, W., and De Vries, J., 2013, The role of climate variation in delta architecture: lessons from analogue modelling: Basin Research, v. 25, p. 1-18.

Blum, M., and Hattier-Womack, J., 2009, Climate change, sea-level change, and fluvial sediment supply to deepwater depositional systems, *in* Kneller, B., Martinsen, O.J., and McCaffrey, W.D., eds., External Controls on Deep Water Depositional Systems: SEPM, Special Publication 92, p. 15-39.

Bourget, J., Zaragosi, S., Rodriguez, M., Fournier, M., Garlan, T., and Chamot-Rooke, N., 2013, Late Quaternary megaturbidites of the Indus Fan: Origin and stratigraphic significance: Marine Geology, v. 336, p. 10-23.

Carvajal, C., 2007, Sediment volume partitioning, topset processes and clinoform architecture - understanding the role of sediment supply, sea level, and delta types in shelf margin building and deepwater sand bypass: the Lance-Fox Hills-Lewis system in S. Wyoming [unpublished PhD thesis]: The University of Texas at Austin, 171 p.

Carvajal, C., and Steel, R., 2012, Source-to-sink sediment volumes within a tectono-stratigraphic model for a Laramide shelf-to-deep-water basin: methods and results, *in* Busby, C., and Azor, A., eds., Tectonics of Sedimentary Basins: Oxford, United Kingdom, Wiley-Blackwell, p. 131-151.

Carvajal, C., and Steel, R., 2009, Shelf-edge architecture and bypass of sand to deep water: influence of shelf-edge processes, sea level, and sediment supply: Journal of Sedimentary Research, v. 79, p. 652-672.

Carvajal, C., and Steel, R.J., 2006, Thick turbidite successions from supply-dominated shelves during sea-level highstand: Geology, v. 34, p. 665-668.

Castelltort, S., and Van Den Driessche, J., 2003, How plausible are high-frequency sediment supply-driven cycles in the stratigraphic record?: Sedimentary Geology, v. 157, p. 3-13.

Catuneanu, O., Abreu, V., Bhattacharya, J.P., Blum, M.D., Dalrymple, R.W., Eriksson, P.G., Fielding, C.R., Fisher, W.L., Galloway, W.E., Gibling, M.R., Giles, K.A., Holbrook, J.M., Jordan, R., Kendall, C.G.St.C., Macurda, B., Martinsen, O.J., Miall, A.D., Neal, J.E., Nummedal, D., Pomar, L., Posamentier, H.W., Pratt, B.R., Sarg, J.F., Shanley, K.W., Steel, R.J., Strasser, A., Tucker, M.E., and Winker, C., 2009, Towards the standardization of sequence stratigraphy: Earth-Science Reviews, v. 92, p. 1-33.

Covault, J.A., Romans, B.W., Graham, S.A., Fildani, A., and Hilley, G.E., 2011, Terrestrial source to deep-sea sink sediment budgets at high and low sea levels: Insights from tectonically active Southern California: Geology, v. 39, p. 619-622.

Crabaugh, J.P., and Steel, R.J., 2004, Basin-floor fans of the Central Tertiary Basin, Spitsbergen: relationship of basin-floor sand-bodies to prograding clinoforms in a structurally active basin, *in* Lomas, S.A., and Joseph, P., eds., Confined Turbidite Systems: Geological Society of London, Special Publication 222, p. 187-208.

Edmonds, D.A., Hoyal, D.C.J.D., Sheets, B.A., and Slingerland, R.L., 2009, Predicting delta avulsions: Implications for coastal wetland restoration: Geology, v. 37, p. 759-762.

Ethridge, F.G., Wood, L.J., and Schumm, S.A., 1998, Cyclic variables controlling fluvial sequence development: Problems and perspectives, *in* Shanley, K.W., and McCabe, P.W., eds., Relative Role of Eustasy, Climate, and Tectonism in Continental Rocks: SEPM, Special Publication 59, p. 17-29.

Frings, R.M., 2008, Downstream fining in large sand-bed rivers: Earth-Science Reviews, v. 87, p. 39-60.

Hampson, G.J., Jewell, T.O., Irfan, N., Gani, M.R., and Bracken, B., 2013, Modest change in fluvial style with varying accommodation in regressive alluvial-to-coastal-plain wedge: Upper Cretaceous Blackhawk Formation, Wasatch Plateau, Central Utah, U.S.A: Journal of Sedimentary Research, v. 83, p. 145-169.

Helland-Hansen, W., and Hampson, G.J., 2009, Trajectory analysis: concepts and applications: Basin Research, v. 21, p. 454-483.

Helland-Hansen, W., Steel, R.J., and Sømme, T.O., 2012, Shelf genesis revisited: Journal of Sedimentary Research, v. 82, p. 133-148.

Holbrook, J., Scott, R.W., and Oboh-Ikuenobe, F.E., 2006, Base-level buffers and buttresses: A model for upstream versus downstream control on fluvial geometry and architecture within sequences: Journal of Sedimentary Research, v. 76, p. 162-174.

Holbrook, J.M., and Bhattacharya, J.P., 2012, Reappraisal of the sequence boundary in time and space: Case and considerations for an SU (subaerial unconformity) that is not a sediment bypass surface, a time barrier, or an unconformity: Earth-Science Reviews, v. 113, p. 271-302.

Kim, W., and Paola, C., 2007, Long-period cyclic sedimentation with constant tectonic forcing in an experimental relay ramp: Geology, v. 35, p. 331.

Kim, W., and Paola, C., Voller, V.R., and Swenson, J.B., 2006, Experimental measurement of the relative importance of controls on shoreline migration: Journal of Sedimentary Research, v. 76, p. 270-283.

Knighton, A.D., 1999, Downstream variation in stream power: Geomorphology, v. 29, p. 293-306.

Koss, J.E., Ethridge, F.G., and Schumm, S.A., 1994, An experimental-study of the effects of base-level change on fluvial, coastal-plain and shelf systems: Journal of Sedimentary Research, v. B64, p. 90-98.

Lisiecki, L.E., and Raymo, M.E., 2005, A Pliocene-Pleistocene stack of 57 globally distributed benthic $\delta^{18}O$ records: Paleoceanography, v. 20, no. PA1003, doi: 10.1029/2004pa001071.

Mackin, J.H., 1948, Concept of the graded river: Geological Society of America, Bulletin, v. 59, p. 463-512.

Martin, J., Cantelli, A., Paola, C., Blum, M., and Wolinsky, M., 2011, Quantitative modeling of the evolution and geometry of incised valleys: Journal of Sedimentary Research, v. 81, p. 64-79.

Martinsen, O.J., Collinson, J.D., and Holdsworth, B.K., 1995, Millstone Grit cyclicity revisited, II: Sequence stratigraphy and sedimentary responses to changes of relative sea-level, *in* Plint, A.G., ed., Sedimentary Facies Analysis: International Association of Sedimentologists, Special Publication 22, p. 305-327.

Martinsen, O.J., Sømme, T.O., Thurmond, J.B., Helland-Hansen, W., and Lunt, I., 2010, Source-to-sink systems on passive margins: theory and practice with an example from the Norwegian continental margin, *in* Vining, B.A., and Pickering, S.C., eds., Petroleum Geology: From Mature Basins to New Frontiers: Proceedings of the 7th Petroleum Geology Conference, Geological Society of London, Petroleum Geology Conference Series, v. 7, p. 913-920.

Miall, A.D., 2013, Fluvial Depositional Systems: Berlin, Springer, 316 p.

Muto, T., 2001, Shoreline autoretreat substantiated in flume experiments: Journal of Sedimentary Research, v. 71, p. 246-254.

Muto, T., and Steel, R.J., 2002a, In defense of shelf-edge delta development during falling and lowstand of relative sea level: Journal of Geology, v. 110, p. 421-436.

Muto, T., and Steel, R.J., 2002b, Role of autoretreat and AS changes in the understanding of deltaic shoreline trajectory: a semi-quantitative approach: Basin Research, v. 14, p. 303-318.

Muto, T., Steel, R.J., and Swenson, J.B., 2007, Autostratigraphy: A framework norm for genetic stratigraphy: Journal of Sedimentary Research, v. 77, p. 2-12.

Muto, T., and Swenson, J.B., 2005, Large-scale fluvial grade as a nonequilibrium state in linked depositional systems: Theory and experiment: Journal of Geophysical Research: Earth Surface, v. 110, no. F03002, doi: 10.1029/2005jf000284.

Muto, T., and Swenson, J.B., 2006, Autogenic attainment of large-scale alluvial grade with steady sea-level fall: An analog tank-flume experiment: Geology, v. 34, p. 161.

Nelson, C.H., Escutia, C., Goldfinger, C., Karabonov, E., Gutierrez-Pastor, J., and De Batist, M., 2009, External controls on modern clastic turbidite systems: Three case studies, *in* Kneller, B., Martinsen, O.J., and McCaffrey, W.D., eds., External Controls on Deep-Water Depositional Systems: SEPM, Special Publication 92, p. 57-76.

Ohmori, H., 1991, Change in the mathematical function type describing the longitudinal profile of a river through an evolutionary process: The Journal of Geology, v. 99, p. 97-110.

Paola, C., Heller, P.L., and Angevine, C.L., 1992a, The large-scale dynamics of grain-size variation in alluvial basins, 1: Theory: Basin Research, v. 4, p. 73-90.

Paola, C., Parker, G., Seal, R., Sinha, S.K., Southard, J.B., and Wilcock, P.R., 1992b, Downstream fining by selective deposition in a laboratory flume: Science, v. 258, p. 1757-1760.

Paola, C., Straub, K., Mohrig, D., and Reinhardt, L., 2009, The "unreasonable effectiveness" of stratigraphic and geomorphic experiments: Earth-Science Reviews, v. 97, p. 1-43.

Petter, A.L., and Muto, T., 2008, Sustained alluvial aggradation and autogenic detachment of the alluvial river from the shoreline in response to steady fall of relative sea level: Journal of Sedimentary Research, v. 78, p. 98-111.

Plink-Björklund, P., and Steel, R., 2002, Sea-level fall below the shelf edge, without basin-floor fans: Geology, v. 30, p. 115-118.

Plink-Björklund, P., and Steel, R., 2005, Deltas on falling-stage and lowstand shelf margins, the Eocene Central Basin of Spitsbergen: Importance of sediment supply, *in* Giosan, L., and Bhattacharya, J., eds., River Deltas-Concepts, Models, and Examples: SEPM, Special Publication 83, p. 179-206.

Plink-Björklund, P., and Steel, R., 2006, Incised valleys on an Eocene coastal plain and shelf, Spitsbergen - part of a linked shelf-slope system, *in* Dalrymple, R.W., Leckie, D.A., and Tillman, R.W., eds., Incised Valleys in Time and Space: SEPM, Special Publication 85, p. 281-307.

Plink-Björklund, P., and Steel, R., 2007, Type II shelf margin, Hogsnyta, Norway: Attached slope turbidite system, *in* Nilsen, T.H., Shew, R.D., Steffens, G.S., and Studlick, J.R.J., eds., Atlas of Deep-Water Outcrops: American Association of Petroleum Geologists, Studies in Geology 56, p. 282-286.

Posamentier, H.W., and Allen, G.P., 1999, Fundamental Concepts of Sequence Stratigraphy, *in* Siliciclastic Sequence Stratigraphy—Concepts and Applications: SEPM, Concepts in Sedimentology and Paleontology 7, p. 9-51.

Posamentier, H.W., and James, D.P., 1993, An overview of sequence-stratigraphic concepts: Uses and abuses, *in* Posamentier, H.W., Summerhayes, C.P., Haq, B.U., Allen, G.P., eds., Sequence Stratigraphy and Facies Associations: International Association of Sedimentologists, Special Publication 18, p. 3-18.

Posamentier, H.W., and Vail, P.R., 1988, Eustatic controls on clastic deposition II - sequence and system tract models, *in* Wilgus, C.K., Hastings, B.S., Kendall, C.G.St.C., Posamentier, H.W., Ross, H.W., and Van Wagoner, J.C., eds., Sea Level Changes - An Integrated Approach: SEPM, Special Publication 42, p. 125-154.

Postma, G., Kleinhans, M.G., Meijer, P.T., and Eggenhuisen, J.T., 2008, Sediment transport in analogue flume models compared with real-world sedimentary systems: a new look at scaling evolution of sedimentary systems in a flume: Sedimentology, v. 55, p. 1541-1557.

Prince, G.D., and Burgess, P.M., 2013, Numerical modeling of falling-stage topset aggradation: Implications for distinguishing between forced and unforced regressions in the geological record: Journal of Sedimentary Research, v. 83, p. 767-781.

Rice, S.P., and Church, M., 2001, Longitudinal profiles in simple alluvial systems: Water Resources Research, v. 37, p. 417-426.

Schumm, S.A., and Lichty, R.W., 1965, Time, space, and causality in geomorphology: American Journal of Science, v. 263, p. 110-119.

Shanley, K.W., and McCabe, P.J., 1994, Perspectives on the sequence stratigraphy of continental strata: American Association of Petroleum Geologists, Bulletin, v. 78, p. 544-568.

Simpson, G., and Castelltort, S., 2012, Model shows that rivers transmit high-frequency climate cycles to the sedimentary record: Geology, v. 40, p. 1131-1134.

Sinha, S.K., and Parker, G., 1996, Causes of concavity in longitudinal profiles of rivers: Water Resources Research, v. 32, p. 1417-1428.

Snow, R.S., and Slingerland, R.L., 1987, Mathematical modeling of graded river profiles: The Journal of Geology, v. 95, p. 15-33.

Sømme, T.O., Helland-Hansen, W., and Granjeon, D., 2009, Impact of eustatic amplitude variations on shelf morphology, sediment dispersal, and sequence stratigraphic interpretation: Icehouse versus greenhouse systems: Geology, v. 37, p. 587-590.

Steel, R., Plink-Björklund, P., and Mellere, D., 2007, Storvola, Type I shelf margin, Norway, *in* Nilsen, T.H., Shew, R.D., Steffens, G.S., and Studlick, J.R.J., eds., Atlas of Deep-Water Outcrops: American Association of Petroleum Geologists, Studies in Geology 56, p. 274-281.

Strong, N., and Paola, C., 2008, Valleys that never were: time surfaces versus stratigraphic surfaces: Journal of Sedimentary Research, v. 78, p. 579-593.

Swenson, J.B., and Muto, T., 2007, Response of coastal plain rivers to falling relative sea-level: allogenic controls on the aggradational phase: Sedimentology, v. 54, p. 207-221.

Van Heijst, M., Postma, G., Van Kesteren, W.P., and De Jongh, R.G., 2002, Control of syndepositional faulting on systems tract evolution across growth faulted shelf margins: An analog experimental model of the Miocene Imo River field, Nigeria: American Association of Petroleum Geologists, Bulletin, v. 86, p. 1335-1366.

Van Heijst, M.W.I.M., and Postma, G., 2001, Fluvial response to sea-level changes: a quantitative analogue, experimental approach: Basin Research, v. 13, p. 269-292.

Voller, V.R., and Paola, C., 2010, Can anomalous diffusion describe depositional fluvial profiles?: Journal of Geophysical Research: Earth Surface, v. 115, no. F00A13, doi: 10.1029/2009jf001278.

Vollmer, S., and Kleinhans, M.G., 2007, Predicting incipient motion, including the effect of turbulent pressure fluctuations in the bed: Water Resources Research, v. 43, no. W05410, doi: 10.1029/2006wr004919.

Wallinga, J., Törnqvist, T.E., Busschers, F.S., and Weerts, H.J.T., 2004, Allogenic forcing of the late Quaternary Rhine–Meuse fluvial record: the interplay of sea-level change, climate change and crustal movements: Basin Research, v. 16, p. 535-547.

Wheeler, H.E., 1964, Baselevel, lithosphere surface, and time-stratigraphy: Geological Society of America, Bulletin, v. 75, p. 599-610.

Wright, S., and Parker, G., 2005a, Modeling downstream fining in sand-bed rivers. I: formulation: Journal of Hydraulic Research, v. 43, p. 613-620.

Wright, S., and Parker, G., 2005b, Modeling downstream fining in sand-bed rivers. II: application: Journal of Hydraulic Research, v. 43, p. 621-631.

9. FIGURE CAPTIONS

Table 1: Input parameters and boundary conditions of the experiments. Q_w and Q_s denote water discharge and sediment discharge, respectively. T and ΔT denote the duration of the experiment and the interval between measurements.

FIG. 1: A) System-scale equilibrium (*sensu* Paola et al. 1992a) is obtained only over geological time scales. The linear equilibrium profile drawn here is idealized (cf. Postma et al. 2008) and will not form in natural systems for multiple reasons but illustrates that all fluvial accommodation is infilled. B) Development of fluvio-deltaic systems on geological time scales. Progradation results in aggradation along the longitudinal profile and prevents these systems from achieving system-scale equilibrium.

FIG. 2: A) Top view of the experiment setup, consisting of two mirror-image models. Sediment and water are added at the sediment feeder. In the fluvial zone no tectonic movement occurs. In the basin, three zones of distinct water depth are formed. Dimensions (mm) are indicated in regular font, gradients in italic font. B) Side view of the experiment, along transect P-P' in part A.

FIG. 3: Input parameters. The water depth is given for the deep zone of the experimental basin; the intermediate and shallow zones of the basin have a water depth of 2/3 and 1/3 of this value. Note that in A) E1_M1, water level and subsidence curves overlay, and in B) E1_M2, the subsidence and water-depth curves overlay, C) E2_M1, D) E2_M2.

FIG. 4: Representation of methods. A) Fill percentage of the longitudinal profile is calculated as the volume percentage of a triangle connecting the upstream and downstream ends of the longitudinal profile (the averaged gradient), and represents a measure of concavity. Increasing fill percentages thus imply that the system becomes less concave. The slope percentage of the longitudinal profile is calculated with reference to an estimated system-scale equilibrium gradient and provides an expression of the longitudinal gradient. See text for discussion of the system-scale equilibrium gradient. B) Sediment bypass is calculated as a percentage between the sediment volume transported past the shoreline of the initial height model, and the total sediment volume between two successive height models. Note the basin geometry and downdip increase in shelf clinoform height (model E1_M1).

FIG. 5: Experiment setup for Scenarios 1 and 2. A) Side view of experiment setup. (1) Position of wide upstream weir. (2) Dry sediment is fed from an overhead sediment feeder. Sediment is deposited on a rough cloth that prevents scouring directly downstream of the upper weir. (3) Downstream weir used in Scenario 1. In Scenario 2, this position indicates the initial shoreline. (4) Pump to recirculate water to the upstream weir. B) Top view of experiment setup. Black plus signs indicate locations for measurement of height models, gray plus signs indicate additional locations during shoreline progradation.

FIG. 6: Quantitative results for E1_M1. A) Input parameters for experiments. Note that the water depth is given for the deep part of the experimental basin; the intermediate and shallow parts of the basin have a water depth of 2/3 and 1/3 of this value. B) Rate of change in relative sea level. C) Width-averaged water depth (mm), calculated along the strike of the clinoform. D) Topset area. E) Progradation rate, calculated between the shoreline of successive height models. F) Sediment

bypass to beyond the shoreline; see Fig. 4B. G) Fill percentage of the longitudinal profile; see Fig. 4A. H) Slope percentage of the longitudinal profile; see Fig. 4A.

FIG. 7: Quantitative results for E1_M2. See description in Fig. 6

FIG. 8A-H: Width-averaged transects through the shallow and deep parts of each experiment. Note that these segments differ mainly in the proximal area of the basin (see Fig. 2A). Each line represents an increment of 8 h during the experiment.

FIG. 9: Quantitative results for E2_M1. A) Input parameters for experiments. Note that the water depth is given for the deep part of the basin; the intermediate and shallow parts of the basin have a water depth of 2/3 and 1/3 of this value. B) Rate of change in relative sea level. C) Water depth (mm) calculated along the strike of the clinoform. D) Topset area. E) Shoreline migration rate, calculated between the shoreline of successive height models. F) Sediment bypass; see Fig. 4B. G) Fill percentage of the longitudinal profile; see Fig. 4A. H) Slope percentage of the longitudinal profile; see Fig. 4A.

FIG. 10: Quantitative results for E2_M2. See description in Fig. 9

FIG. 11: Photographs of the topset morphology of E2_M1 during sea-level cycle 3. A) Highstand normal regression; the entire surface area of the topset is frequently wetted. B) Early rorced regression; small interfluves emerge that are regularly eroded. C) Incised-valley formation during late forced regression began at the shoreline of the deep zone of the experimental basin. D) Lateral migration of the incised-valley mouth after significant progradation of the shoreline widens the

incised valley. E) Transgression of the distal topset, resulting in a back-stepping coastline. Continued upstream migration of erosion initiated by the previous sea-level fall increases the diachroneity of the sequence boundary.

FIG. 12: Erosion-deposition maps for E2_M1. Blue and red indicates respectively deposition and erosion; increasing color intensity indicates increasing magnitude. Gray contour lines are spaced at 10 mm vertical intervals and indicate topography at the end of the mapped interval. Yellow contour line represents the shoreline. A) Lowstand 1 (8 – 16 h), relatively minor erosion and rapid progradation into the shallow zone of the experimental basin. B) Transgression 1 (16 – 24 h), deposition occurs along the entire longitudinal profile. C) Lowstand 3 (56 – 64 h), erosion is more severe and has migrated far upstream. Less progradation occurs than in lowstand 1 due to the significant increase in water depth. D) Transgression 3 (64 – 72 h), erosion related to the previous sea-level fall continues updip during the entire sea-level rise while the coastline is characterized by back-stepping lobes on the lowstand shelf.

FIG. 13. Longitudinal gradients and downstream-fining trends for Scenarios 1 and 2. A) Longitudinal profiles for Scenario 1 through time. The final profiles overlay each other, implying full sediment bypass along a system-scale equilibrium gradient. The dashed line represents initial bed height and position of weir. B) Sediment samples collected along the final longitudinal profile of Scenario 1 indicate that the coarse-grained fraction (> 1 mm) is represented along the entire profile without a clear downstream-fining trend. C) Grain-size samples collected below the downstream weir from 0 to 4 h are depleted of coarse-grained fraction, indicating downstream fining. From 4.5 h onwards, input and output of coarse-grained sediment (> 1 mm) are roughly equal, indicating that no downstream fining occurs. The peak in coarse-grained sediment (6.5 h) might indicate progradation of a gravel front that accumulated upstream during the earlier stages of the experiment. D)

Longitudinal profiles for Scenario 2. Dashed line indicated by E indicates the water level and initial bed height. Scenario 2 aggrades to a substantially lower gradient than Scenario 1 while upstream conditions are equal. E) Grain-size samples collected along the final longitudinal profile indicate that the coarse fraction (> 1 mm) is mainly retained in the steep, proximal part of the system (0 – 2 m).

FIG. 14: Influence of water depth on the longitudinal grade of sedimentary systems. Gradients and curvature are exaggerated. A) In a system of fixed length, a system-scale equilibrium profile can develop in which the sediment input is equal to the sediment output. B) In sedimentary systems prograding into shallow-water basins, high progradation rates lead to strongly concave, low-gradient longitudinal profiles in which coarse sediment is largely retained upstream. Large sediment volumes are sequestered in the relatively high accommodation fluvial system. C) The longitudinal profile of fluvio-deltaic systems prograding into deeper water can approach system-scale equilibrium more closely because of low progradation rates, resulting in high sediment transport rates to the coastline and limited downstream fining. D) Fluvio-deltaic systems prograding into deepening water in ramp-style settings will approach system-scale equilibrium more closely, gradually increasing sediment bypass to the shoreline and decreasing in downstream fining. E) Relative sea-level fall in shallow-water systems or on a shelf. Rapid progradation will impede erosion, but sea-level fall is still likely to increase the gradient and decrease the concavity of the longitudinal profile, increasing the efficiency of sediment transport along the longitudinal profile and reducing downstream fining. F) In moderate water depths, for example shelf clinoforms of small height, relative sea-level fall can lead to significant erosion and high sediment bypass beyond the shoreline during late falling stage and lowstand. G) The likelihood of valley incision depends on the rate and amplitude of sea-level fall but also increases with increasing water depth. Valley incision can result a lowering the system-scale equilibrium gradient within the incised valley. H) Sea-level rise results in an increased concavity of the longitudinal profile and strong downstream fining, resulting in fine-grained highstand systems aggrading on the lowstand shelf deposits.

FIG. 15: A) Clinothem succession of the Maastrichtian Lance - Fox Hills – Lewis shelf margin, southern Wyoming. Note that the aggradational succession in Stage 1 (C1-C9) represents a relative sea-level rise, and Stage 2 (C10-C15) a progradational succession during relative sea-level stillstand. Simplified from Carvajal and Steel (2006). B) Sand/shale ratios for individual clinothems, modified from Carvajal (2007). C) Alternative interpretation of sediment volume and grain-size trends, with strongly exaggerated gradients in which the differences in sediment supply and grain size are attributed to the response of the longitudinal profiles to changes in water depth and basin development.

	Q_w (m^3h^{-1})	Q_s (m^3h^{-1})	T (h)	ΔT (h)	Boundary conditions varied
E1_M1	1	0.004	96	8	Water depth
E1_M2	1	0.004	96	8	Water depth and subsidence
E2_M1	1.5	0.004	72	8	Water depth, subsidence, and sea-level variation
E2_M2	1	0.004	72	8	Water depth, subsidence, and sea-level variation
Scenario 1	5.5	0.007	8	0.5	Basin with constraining weir, no progradation
Scenario 2	5.5	0.007	8	0.5	Shallow-water progradation (3 cm)

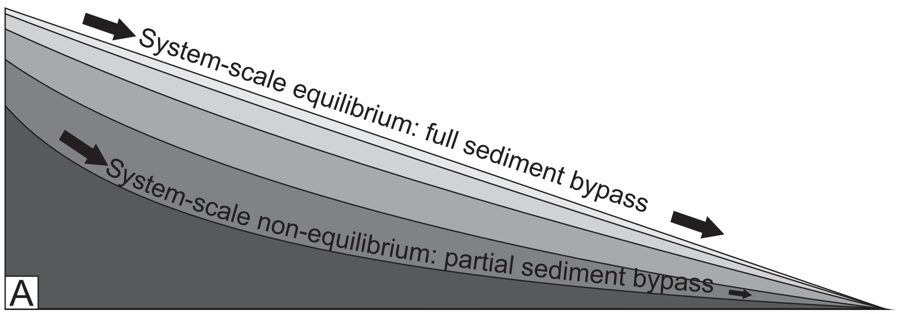

System-scale equilibrium (*sensu* Paola et al. 1992a; Muto and Swenson 2005)

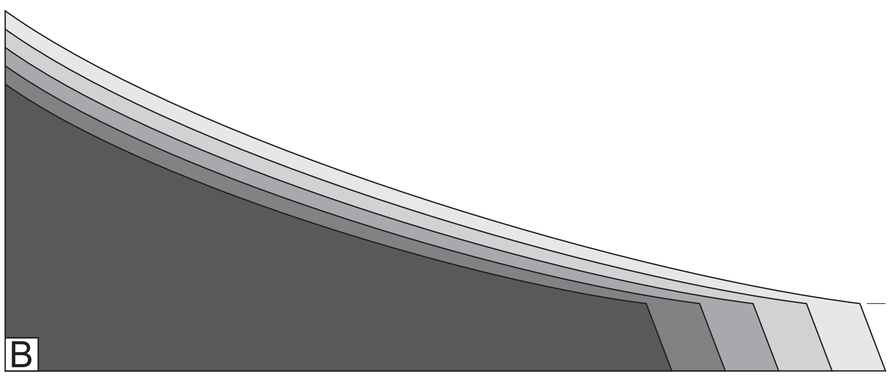

Progradation with constant relative sea level resulting in fluvial aggradation (*sensu* Muto and Swenson 2005)

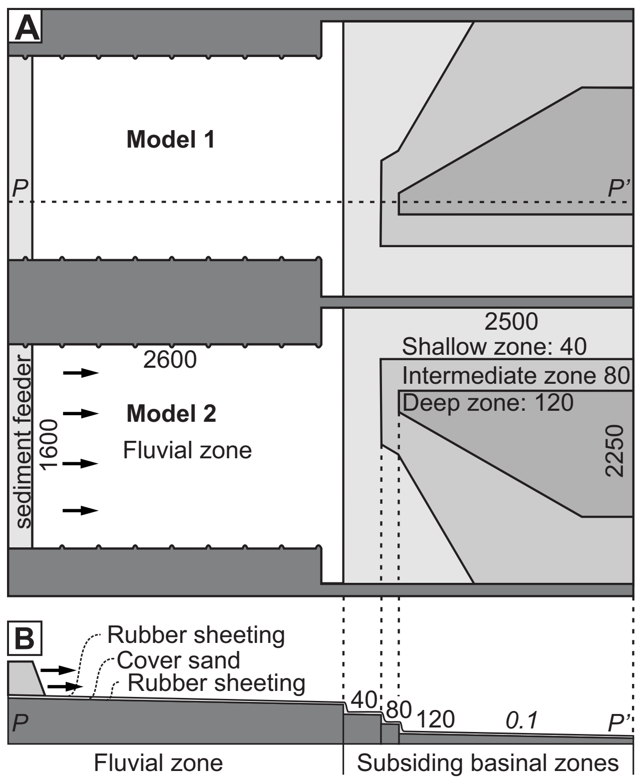

A
Model 1
P
P'
2500
Shallow zone: 40
Intermediate zone 80
Deep zone: 120
2600
Model 2
Fluvial zone
sediment feeder
1600
2250
B
Rubber sheeting
Cover sand
Rubber sheeting
40
80
120
0.1
P
P'
Fluvial zone
Subsiding basinal zones

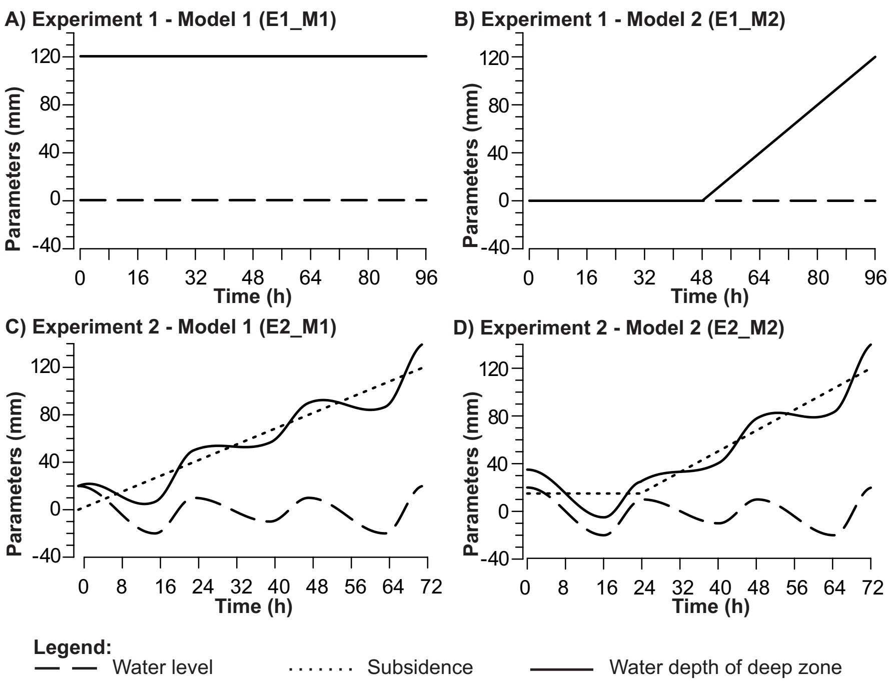
A) Experiment 1 - Model 1 (E1_M1)
B) Experiment 1 - Model 2 (E1_M2)
C) Experiment 2 - Model 1 (E2_M1)
D) Experiment 2 - Model 2 (E2_M2)
Parameters (mm)
Time (h)
Legend:
Water level
Subsidence
Water depth of deep zone

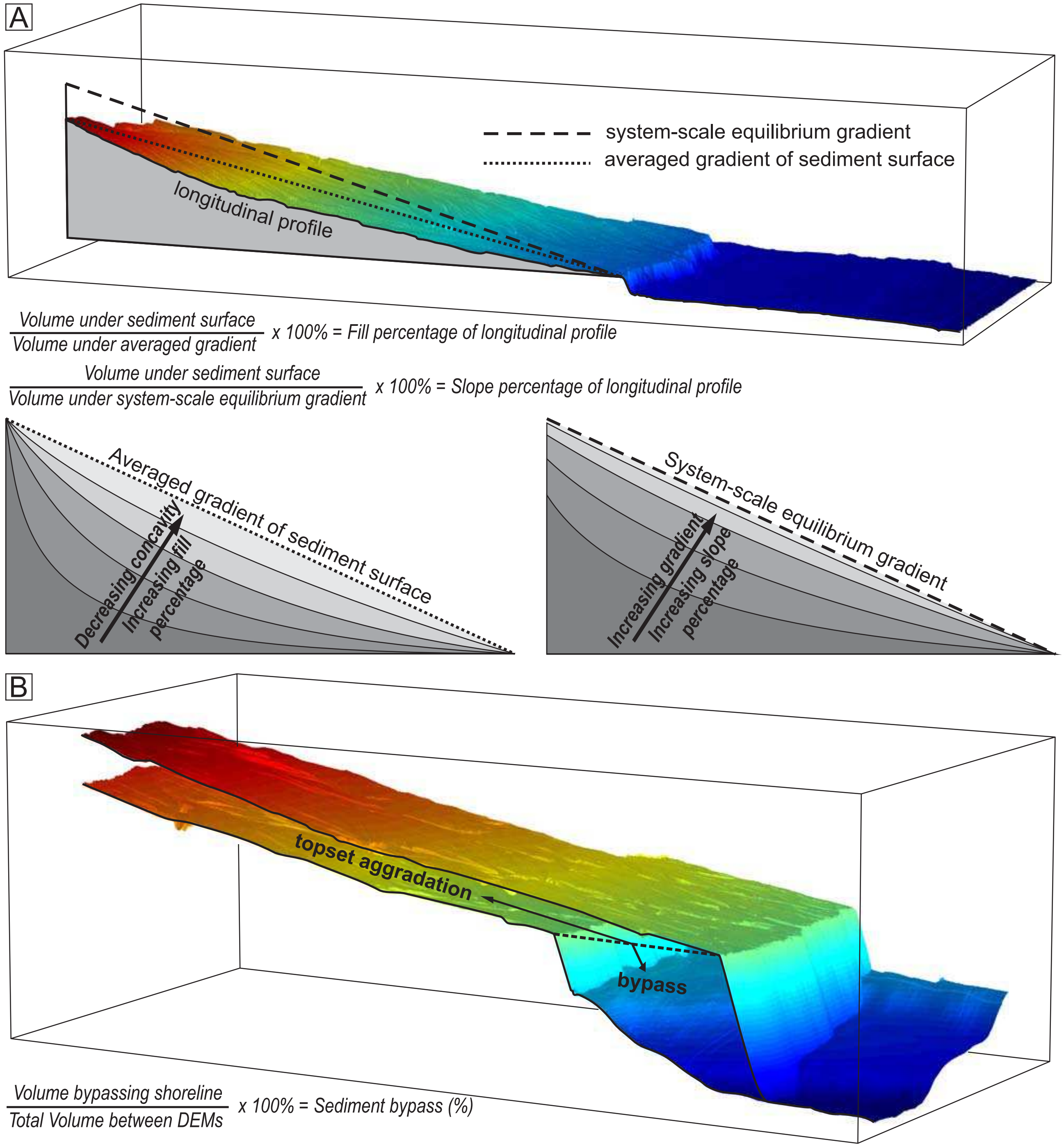
A
system-scale equilibrium gradient
averaged gradient of sediment surface
longitudinal profile
Volume under sediment surface / Volume under averaged gradient x 100% = Fill percentage of longitudinal profile
Volume under sediment surface / Volume under system-scale equilibrium gradient x 100% = Slope percentage of longitudinal profile
Averaged gradient of sediment surface
Decreasing concavity
Increasing fill percentage
System-scale equilibrium gradient
Increasing gradient
Increasing slope percentage
B
topset aggradation
bypass
Volume bypassing shoreline / Total Volume between DEMs x 100% = Sediment bypass (%)

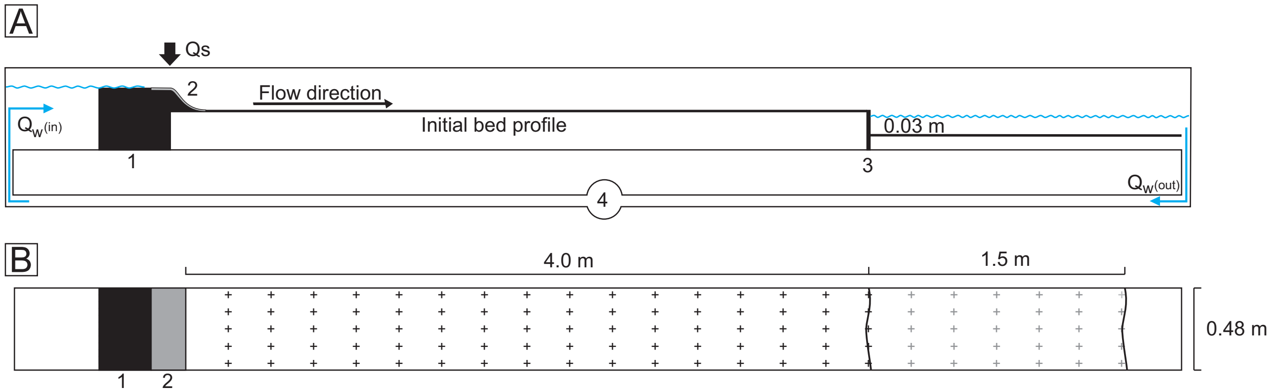
A
Qs
2
Flow direction
Initial bed profile
$Q_{w(in)}$
0.03 m
1
3
4
$Q_{w(out)}$
B
4.0 m
1.5 m
0.48 m
1
2

Figure 6) Experiment 1 - Model 1 (E1_M1)

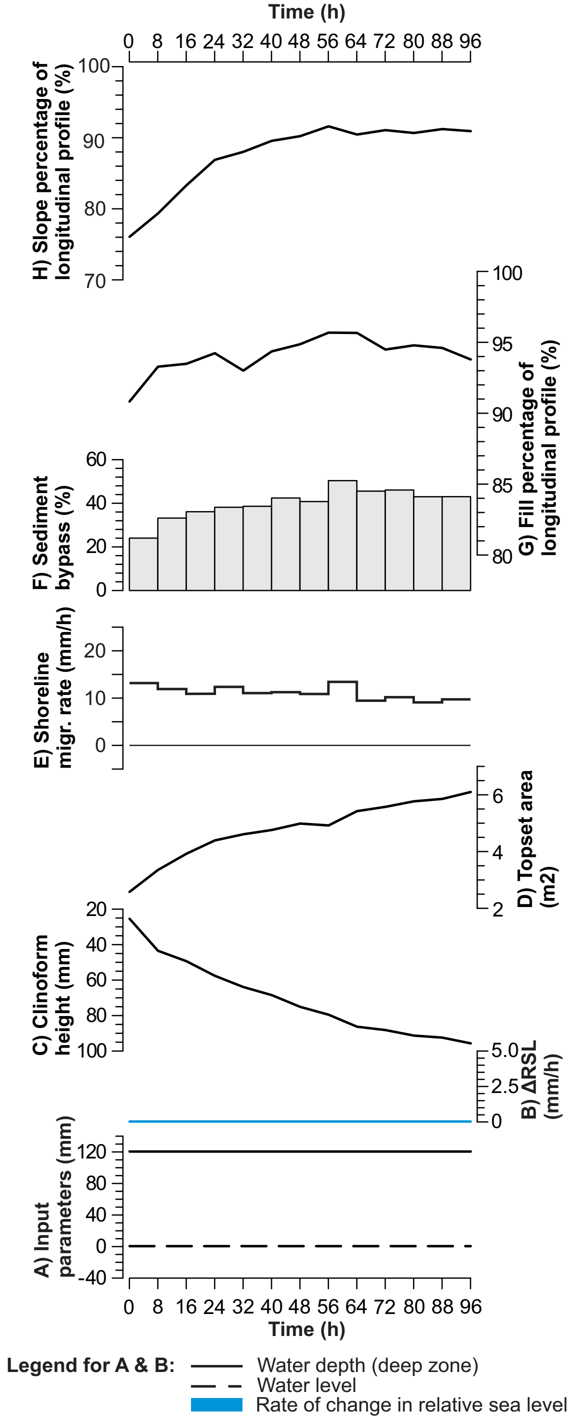

Figure 7) Experiment 1 - Model 2 (E1_M2)

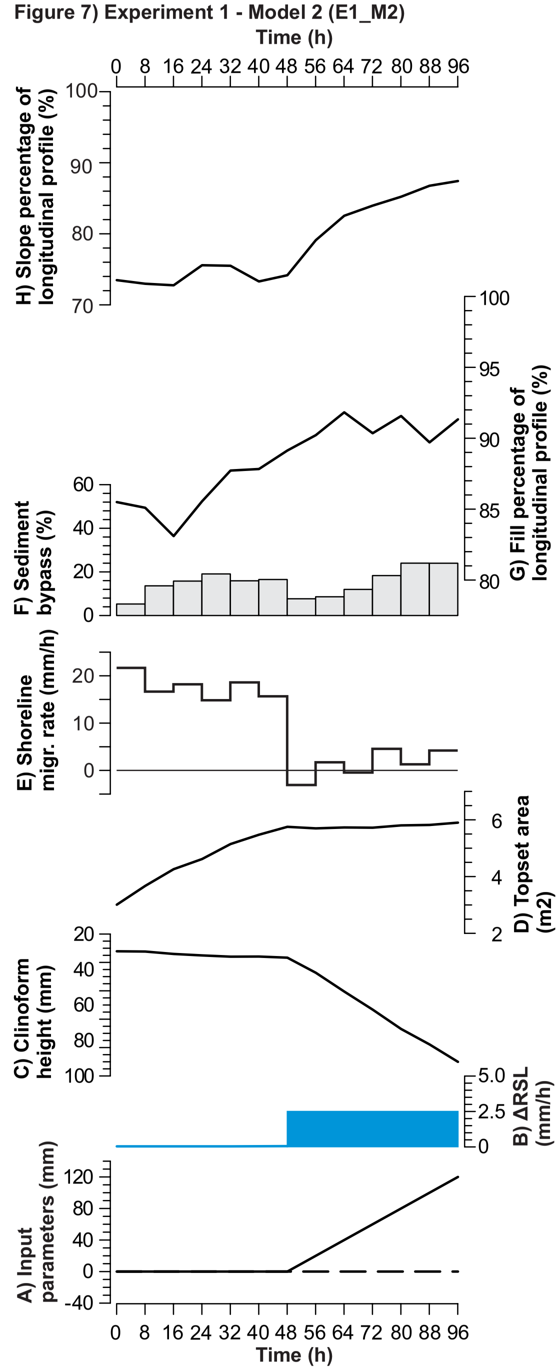

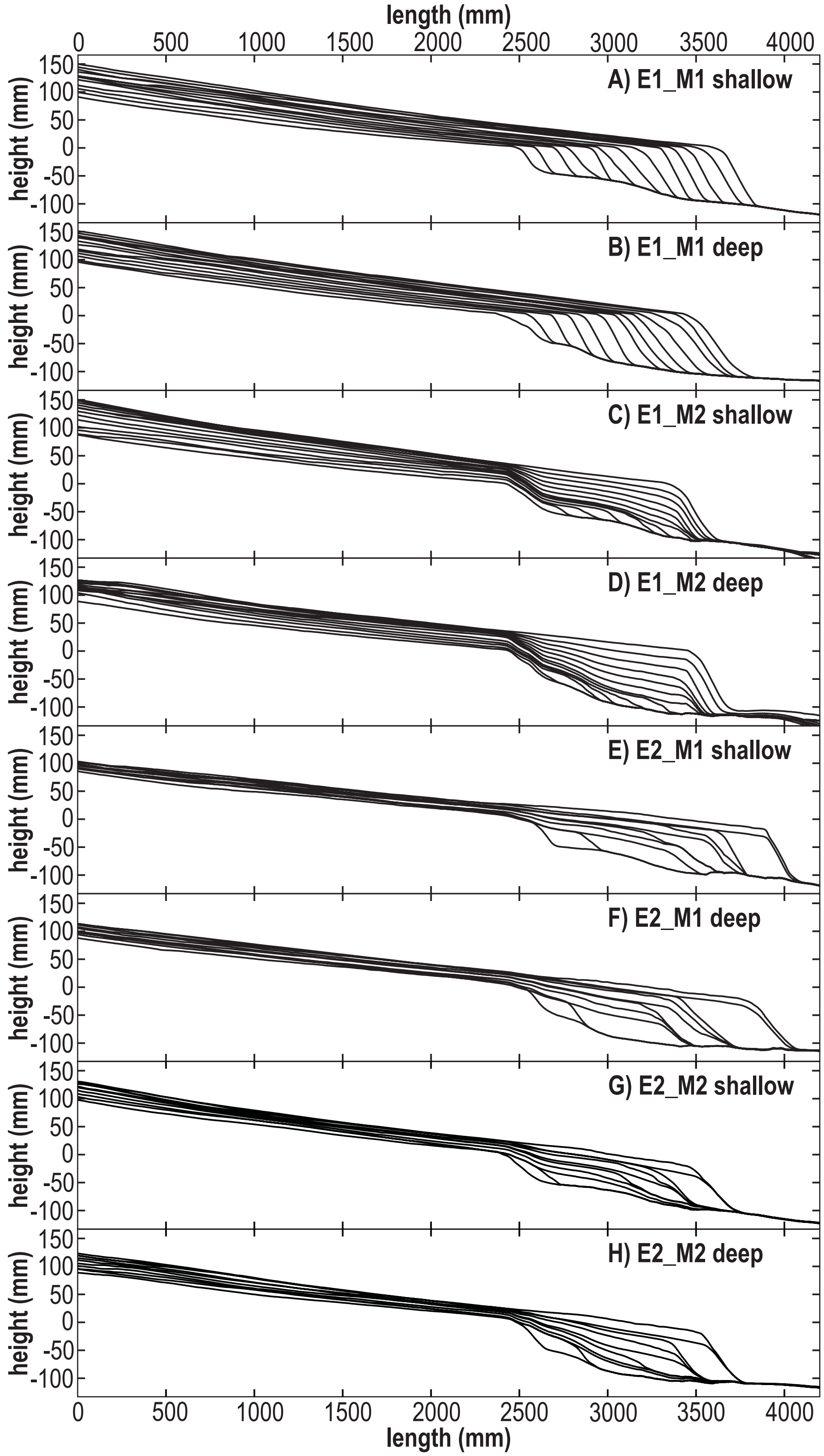
length (mm)
0
500
1000
1500
2000
2500
3000
3500
4000
height (mm)
150
100
50
0
-50
-100
A) E1_M1 shallow
B) E1_M1 deep
C) E1_M2 shallow
D) E1_M2 deep
E) E2_M1 shallow
F) E2_M1 deep
G) E2_M2 shallow
H) E2_M2 deep

Figure 9) Experiment 2 - Model 1 (E2_M1)

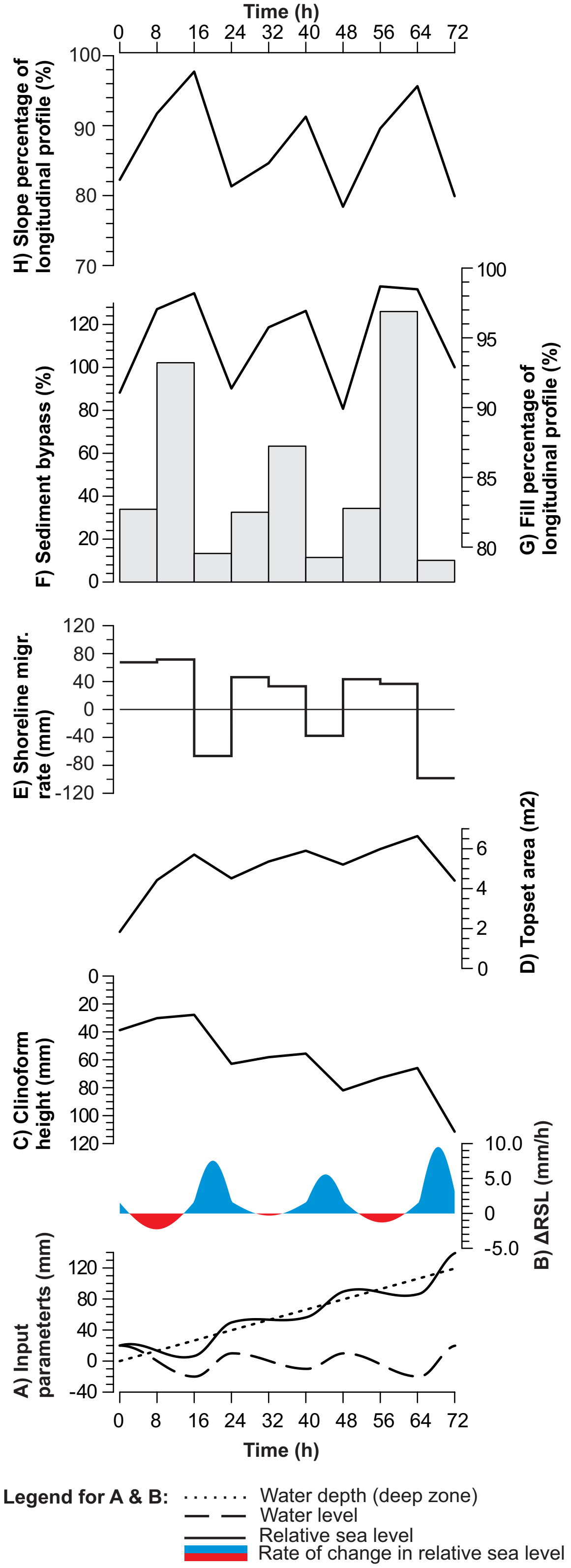

Figure 10) Experiment 2 - Model 2 (E2_M2)

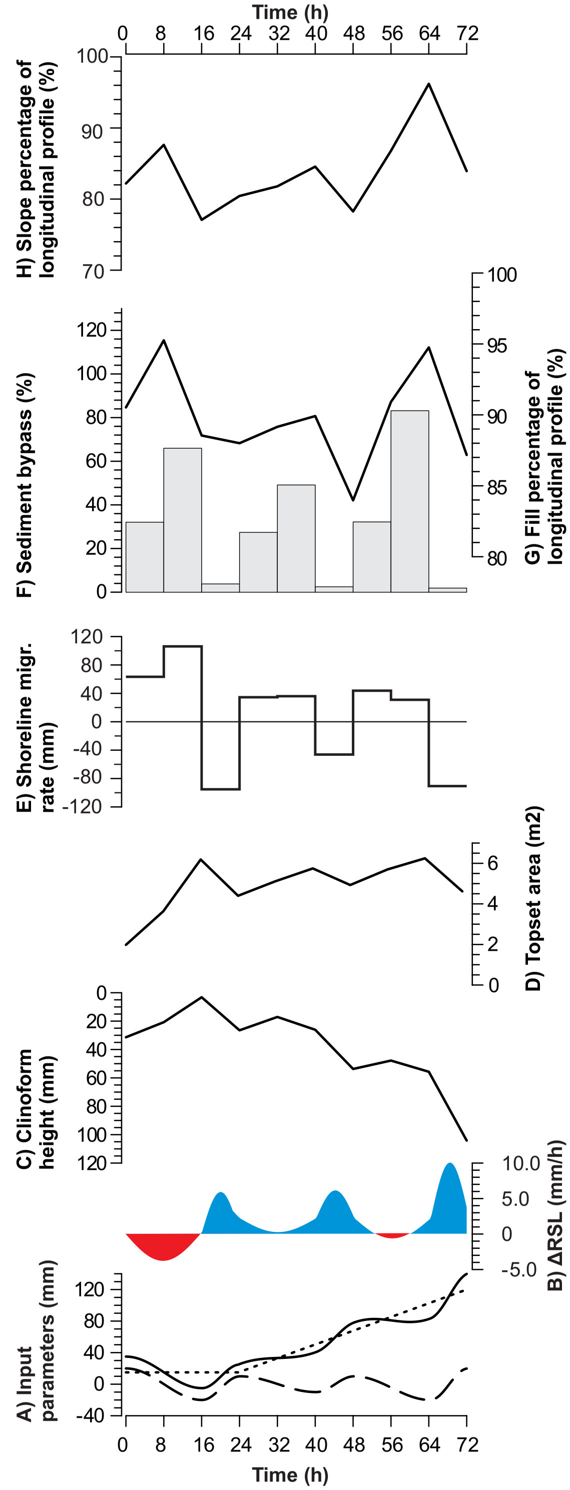

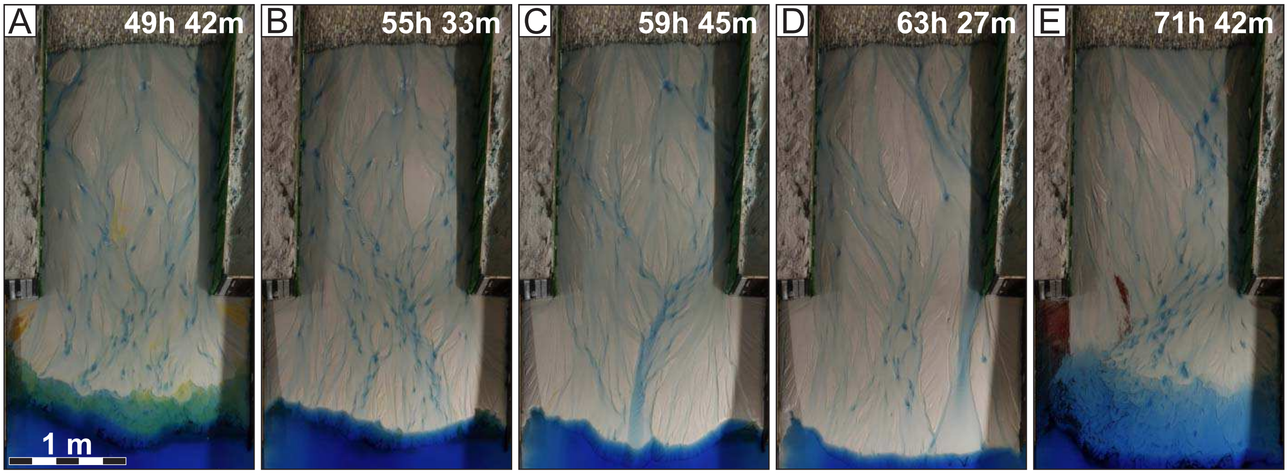
A
49h 42m
1 m
B
55h 33m
C
59h 45m
D
63h 27m
E
71h 42m

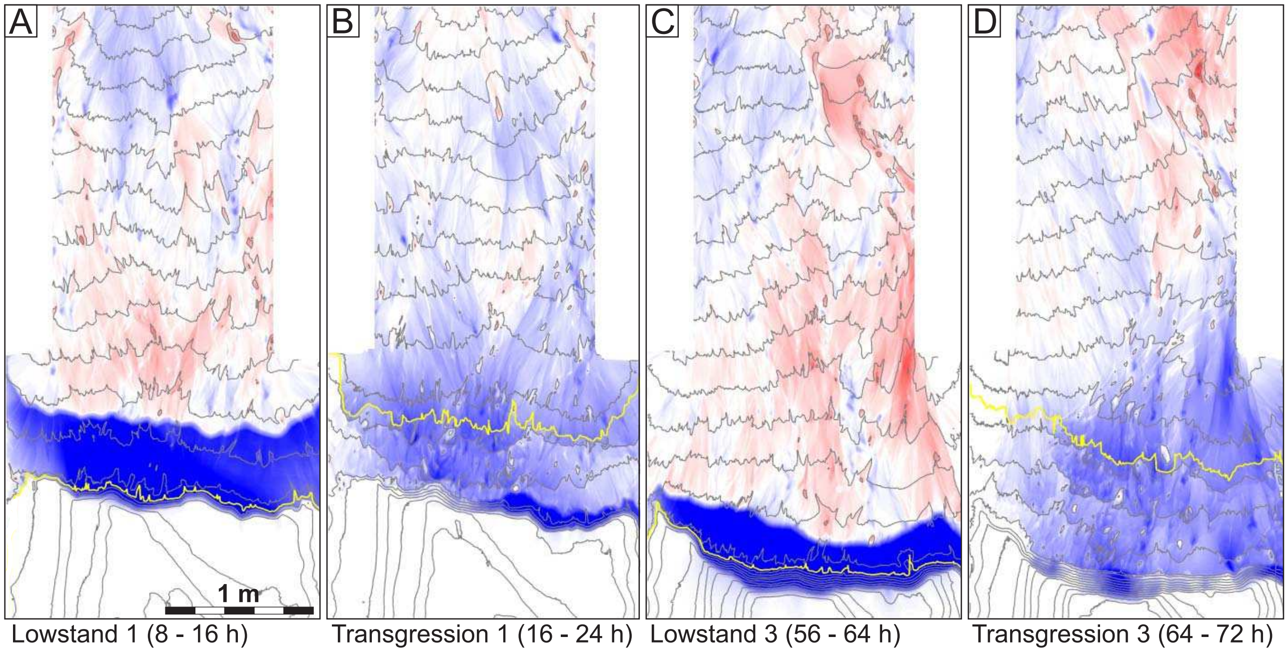
A
B
C
D
1 m
Lowstand 1 (8 - 16 h)
Transgression 1 (16 - 24 h)
Lowstand 3 (56 - 64 h)
Transgression 3 (64 - 72 h)

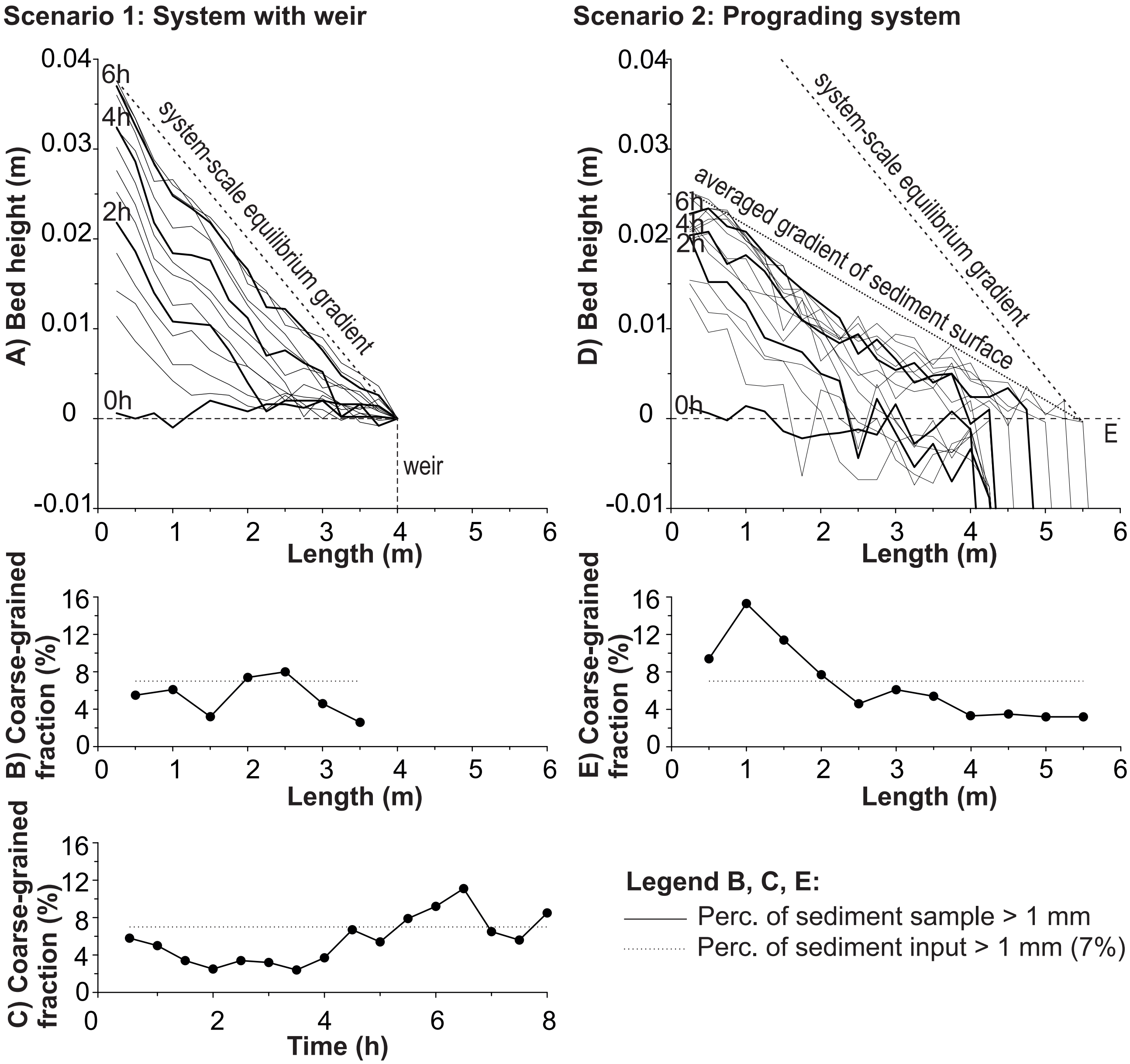

Scenario 1: System with weir
Scenario 2: Prograding system
A) Bed height (m)
system-scale equilibrium gradient
6h
4h
2h
0h
weir
Length (m)
D) Bed height (m)
averaged gradient of sediment surface
E
B) Coarse-grained fraction (%)
E) Coarse-grained fraction (%)
C) Coarse-grained fraction (%)
Time (h)
Legend B, C, E:
Perc. of sediment sample > 1 mm
Perc. of sediment input > 1 mm (7%)

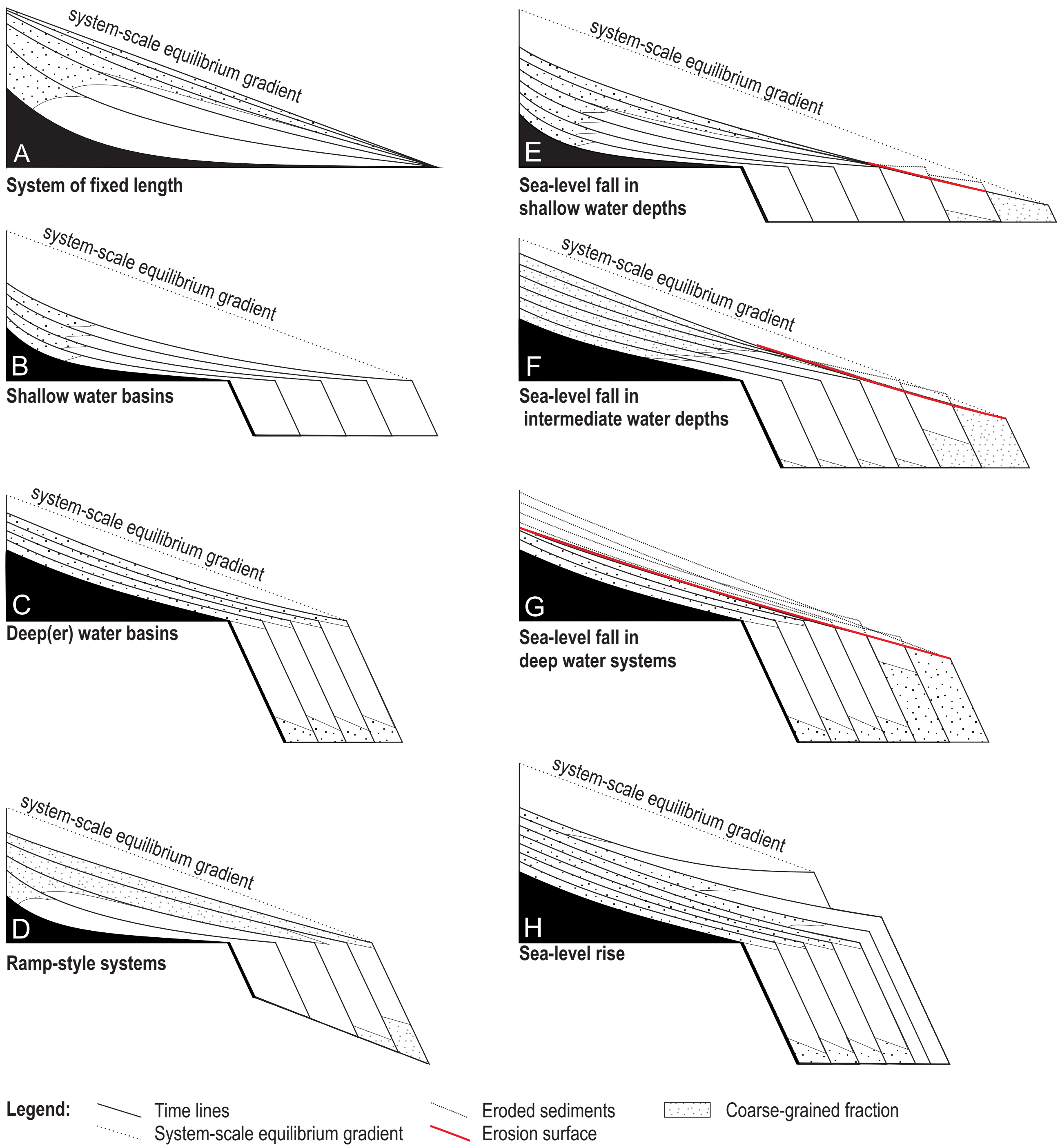
system-scale equilibrium gradient
A
System of fixed length
B
Shallow water basins
C
Deep(er) water basins
D
Ramp-style systems
E
Sea-level fall in
shallow water depths
F
Sea-level fall in
intermediate water depths
G
Sea-level fall in
deep water systems
H
Sea-level rise
Legend:
Time lines
System-scale equilibrium gradient
Eroded sediments
Erosion surface
Coarse-grained fraction

A

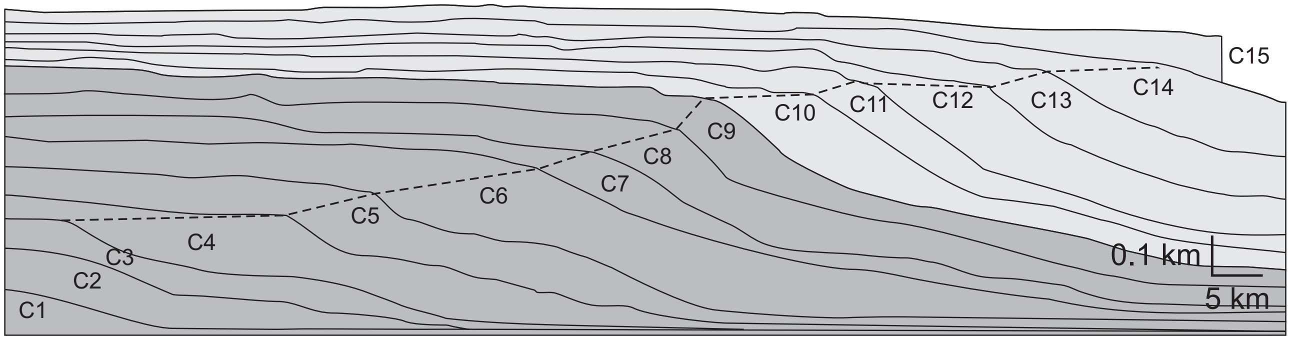
C15
C14
C13
C12
C11
C10
C9
C8
C7
C6
C5
C4
C3
C2
C1
0.1 km
5 km

B

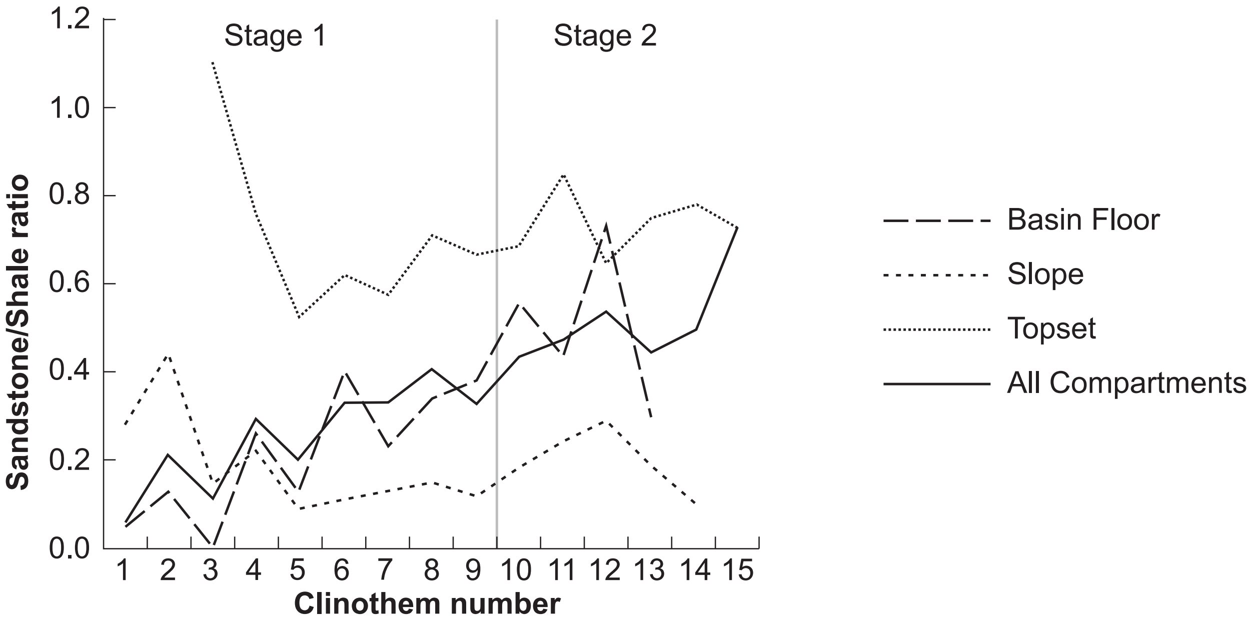
Stage 1
Stage 2
Sandstone/Shale ratio
1.2
1.0
0.8
0.6
0.4
0.2
0.0
1
2
3
4
5
6
7
8
9
10
11
12
13
14
15
Clinothem number
Basin Floor
Slope
Topset
All Compartments

C

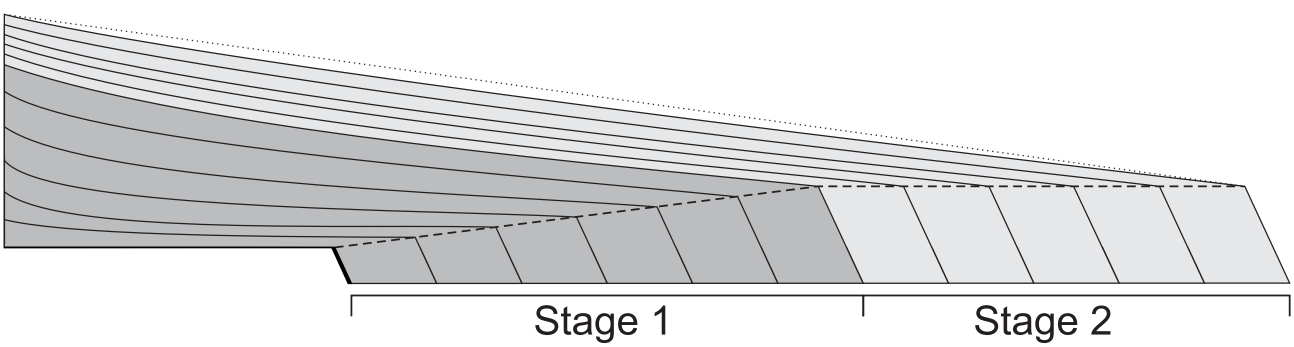
Stage 1
Stage 2